



# Technology for condition and performance evaluation of highway bridges

Shi Ye<sup>1</sup> · Xiangang Lai<sup>1</sup> · Ivan Bartoli<sup>1</sup> · A. Emin Aktan<sup>1</sup>

Received: 30 December 2019 / Revised: 15 April 2020 / Accepted: 23 April 2020 / Published online: 10 May 2020  
© Springer-Verlag GmbH Germany, part of Springer Nature 2020

## Abstract

Today, bridge owners must consider increasing traffic demands (in both volume and weight) and also face concerns related to sustainability, resilience and liveability which were virtually unknown in the 1950s. Furthermore, legislators demand data-driven asset management decisions based on objective, quantitative and reliable bridge condition and performance evaluation. To explore the current state-of-the-art in objective performance and condition evaluation of constructed systems by leveraging technology, a 30-year old freeway bridge in New Jersey, exhibiting multiple complex performance deficiencies, was transformed into a field laboratory. To identify the root causes of performance concerns, Visual Inspection, Operational Monitoring, Forced Excitation Testing, Controlled Load Testing, Non-destructive Probes, Long-term Monitoring, Finite Element Modelling and Parameter Identification were conducted within a Structural Identification framework. The results showed that root causes of some performance deficiencies of the test bridge were identified definitively only through the application of field measurements and analyses integrated by following a scientific approach—i.e. Structural Identification. Controlled Proof-Load Testing was especially useful in demonstrating the location and impacts of damage and the remaining capacity although such an approach can only be considered for the most critical cases due to its high cost and disruption to operations. Operational monitoring was shown as a sufficient and much cheaper alternative for structural identification permitting the development of a 3D digital twin of the bridge, which proved critical in identifying the root causes of its deficiencies and formulating meaningful interventions. Without an a-priori model used for designing the experiments as well as a model (i.e. a digital twin) calibrated by parameter identification and used for simulations, it was not possible to offer options for corrective measures confidently. The study demonstrated the challenges in relying only on visual inspection when a multitude of interdependent mechanisms lead to damage and deterioration, and the information value of different experimental methods such as vibration testing, proof load testing, wide-area NDE scans and multi-year SHM in being able to understand the root causes of various damages.

**Keywords** Condition and performance evaluation · Structural health monitoring · Structural identification · Vibration testing · Controlled load testing · Non-destructive evaluation · Finite element model updating

## 1 Introduction

Nearly 40% of the United States (US) bridges were built over 50 years ago which corresponds to their design-life. The average age of bridges labelled as “Structurally Deficient” in the Federal Highway Administration’s (FHWA) National Bridge Inventory is 62 years [1]. Managing such a significantly aging bridge population requires tools to reliably assess the performance, condition and remaining life of these structures based on objective data that can lead to optimum asset management. In this context, transportation stakeholders face increasingly complex decisions for repair, retrofit or renewal of their critical

---

✉ Shi Ye  
shi.ye@drexel.edu  
Xiangang Lai  
xl388@drexel.edu  
Ivan Bartoli  
ibartoli@drexel.edu  
A. Emin Aktan  
aaktan@drexel.edu

<sup>1</sup> Department of Civil, Architectural and Environmental Engineering, Drexel University, Philadelphia, PA, USA

assets. Different technology tools that can provide objective condition evaluations have become available but given the inertia in the practice of bridge engineering and a lack of fully understanding the challenges to their reliable applications, they are not yet widely incorporated. Consequently, management decisions are still primarily made without leveraging objective measurement data and without a complete mechanistic understanding of bridge behaviour and performance. Bridge engineering practice must transition to performance and condition evaluation tools offering objective and quantitative information that will enable sound decisions regarding bridge-foundation-soil serviceability, durability, safety and stability, remaining life as well likely failure modes which may be significantly affected by deterioration and damage. This requires minimum standards and best practice guidelines and this study was intended to serve as an example.

Visual inspection has served as the standard practice for highway bridge condition evaluation for fifty years, and is intended for collecting information on observable conditions (such as corrosion, cracks, spalls, excessive deformations and vibration); and possibly observe/deduce the causes (such as trapped water, salt, temperature effects, live loads, wind, settlement and others) leading to deterioration. Bridge inspection costs increase as the size and complexity of a bridge increases, starting from \$tens of Thousands for typical highway overpasses and reaching \$tens of Millions for major long-span bridges. Considering the replacement cost of most highway bridges may range between \$10's of Millions to \$Billions, there are great advantages in improving the reliability and information content of visual inspections and perhaps even reduce their frequency, if justified. Indeed, the recently proposed changes to the National Bridge Inspection Standards by the FHWA (2020) encourage technology adoption (e.g. Unmanned Aerial Vehicles, UAVs) and permits reducing the frequency of inspections if warranted by the attributes of a bridge.

Advancing emerging technologies (such as the Cloud, UAVs), Robotics, Machine Learning and Computer Vision) are being explored to support visual inspection. Despite this, visual inspections have known limitations in addition to their subjectivity; for instance, unless an inspector is an experienced bridge structural engineer who can understand the vulnerabilities due to a bridge's alignment, approaches, geometry, super-and-sub-structures, foundations and soil as a SYSTEM, "it is too easy and common to miss the forest because of the trees." The inspector has to recognize patterns of deterioration and distress, their likely causative mechanisms, and understand how any observed deterioration, damage or anomaly in performance may impact the safety and lifecycle of a bridge, based on its spans, redundancies, discontinuities, bearings and sub-structural systems in addition to foundations, soil and hydraulics.

Unfortunately, most inspectors, irrespective of their degrees, licensing or credentials, cannot recognize unknown reserve capacities nor discover deficiencies that are not visible (e.g. initiation of fatigue cracking, frozen movement systems or a delaminated deck) which leads to much uncertainty in deciding on the actual condition, performance and safety of an existing bridge. The limitations in the human ability to observe the entirety of a bridge system at a moment in time, and project its performance into the future are well-known. Furthermore, most inspectors are not engineers and are trained to follow a checklist. While we cannot deny the value of decades of accumulated heuristic knowledge of a handful of bridge designers and engineers, their numbers are not sufficient to inspect over 600,000 bridges. To circumvent such deficiencies, several technologies in the realm of Operational Monitoring, Forced Vibration testing, Load-Testing, Non-Destructive Evaluation (NDE) and Structural Health Monitoring (SHM) have been proposed but many questions remain before their implementation can become reliable and widely considered by bridge owners.

Important questions to consider before bridge owners find it worthwhile to invest into technology include: (1) how can bridge managers select the proper technology tools while minimizing the cost and time needed to adopt the selected technologies and collect reliable data pertinent for the effective management of their assets? (2) What is the cost and information value of data from different types of field experiments and analytical/numerical modelling approaches? How can we evaluate the reliability of experimental data and the outcomes of analytical/numerical simulations by a-priori as well as calibrated analytical models? (3) What are the challenges in identifying the root causes of performance deficiencies caused by design, construction, operations and maintenance errors, and which technologies are cost-effective for identifying these? (4) What is the influence of dynamics in the performance of bridges? What are the attributes that may lead to large amplification in stresses? Since common bridges are designed by considering them as single-line girders, and ignoring their 3D dynamic behaviour, there is a pressing need to understand their behaviour as 3D systems including bearings, substructures, foundations and soil.

The objective of this study was to seek answers to some of the above questions. The study was designed to discover which technologies and their integration strategies are reliable and necessary to identify the root causes of bridge performance concerns as a step towards objective bridge condition and performance evaluation. For this reason, a 30-Year old highway bridge with multiple simple spans featuring a reinforced concrete deck on steel girders and exhibiting a multitude of performance deficiencies was provided by NJDOT as a test specimen, importantly characterized as a "Nightmare Bridge" by the state bridge engineer due to its

exhibiting many types of interdependent deterioration and damage (Fig. 1).

The structural system of the test bridge and its design is a common one throughout the US highway system. Various field experiments were conducted on the same span during 2012–2013 with the participation of experienced bridge engineers and bridge research experts from Japan, Korea, the United Kingdom, Austria, Switzerland and the US. The study was funded by the USDOT–FHWA and NJDOT as a part of the FHWA’s Long-Term Bridge Performance Study, and it was coordinated by Drexel University with participation from Rutgers and Princeton University.

In this study, Structural Identification was leveraged for integrating various experimental tools for bridge condition assessment. The technologies involved sensing, imaging, traffic induced or controlled excitation as well as controlled proof-level truck-loading, Finite Element (FE) modelling, parameter identification, simulation and other tools in the realm of information technology. Experiences in the application of these tools in conjunction with the fundamental steps of St-Id are discussed and evaluated in the following.

## 1.1 Structural identification

Structural Identification (St-Id) has been explored as a tool to study the actual behaviour of buildings and bridges for many years [2]. St-Id seeks a mechanistic and quantitative description of a structural system in the context of a physics-based

FE model i.e. a digital twin. The best practices for St-Id were summarized as a six-step analysis-experiment-decision integration cycle by the ASCE St-Id of Constructed Systems Committee [3]: (1) observation and conceptualization; (2) a-Priori modelling; (3) controlled experimentation; (4) processing and interpretation of data; (5) model calibration and parameter identification; and (6) utilization of the calibrated model i.e. digital-twin for simulations and decision-making.

The *first step* of St-Id involves observing all concerns and issues that are driving the application, followed by a sound business-case, as well as conceptualizing the structure. Advanced tools and technologies such as 3D Bridge Info Modelling (BRIM), data mining and computer vision technologies that may be employed in this step may improve the efficiency of information collection. To properly guide the application of St-Id, it is critical to assign a coordinator who would follow and integrate all of the Six Steps [2], and identify potential uncertainties associated with construction and history, loading mechanisms, kinematics, and critical intrinsic forces due to construction and environmental inputs.

In the *second step*, an a-priori 3D Finite Element model of the entire structure-foundation-soil system is drafted based on the information collected in the first step, and this model is utilized to aid in the selection of appropriate experimental approaches, sensors, instrumentation and data acquisition as well as data quality assurance plans to execute the following step. Many bridge engineers may not recognize the importance of an a-priori model, and they may believe

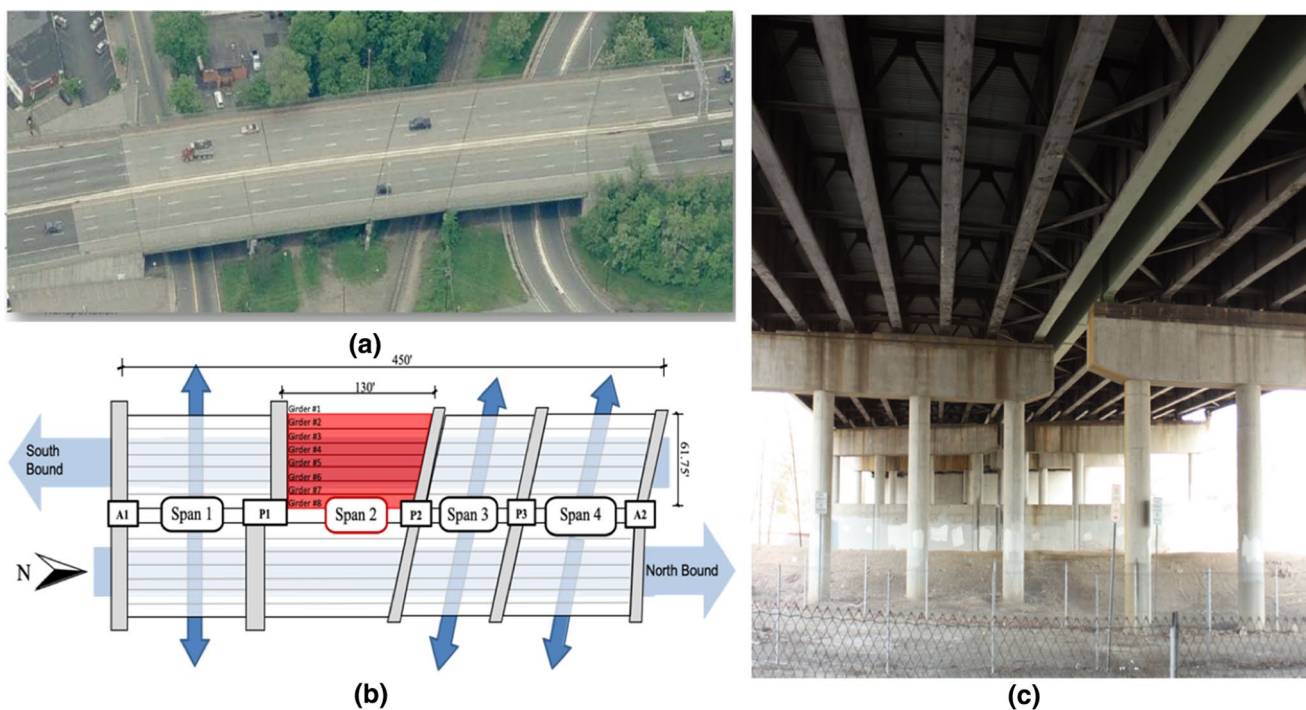


**Fig. 1** The selected bridge: (a) view captured from Google Maps; (b) site layout; (c) photo showing superstructure and substructure

a field test or other experiment may be designed based on heuristics alone. Such an approach short-cuts the scientific method: OBSERVE-HYPOTHESE-TEST-PROVE/DISPROVE HYPOTHESIS, going back to Plato (429–347 BC) and often leads to unreliable results given the levels of uncertainty in properly simulating the behaviour of a complex and deteriorated system. Constructing an a-priori model helps to conceptualize a bridge and identify the principal mechanisms of uncertainty and how experiments may be designed to reduce the uncertainty.

Although sensing and information technologies have significantly improved in the last decade, *Step three* still involves trade-offs to ensure the accuracy and reliability of acquired data without significant and sometimes unnecessary cost. The *fourth step* involves the processing and interpretation of the experimental data. This step invariably aims to control and remove data errors and noise (averaging, windowing, filtering), extract key response indices, and plot such indices temporally and spatially (response versus load position, load level, frequency, etc.) to facilitate effective visualization and interpretation. Once the data has been effectively validated, reduced and interpreted, the preliminary model is then calibrated in *Step five* to minimize its discrepancies with the experiment.

A calibrated model by leveraging *heuristics and data* as a product of St-Id can help bridge engineers reduce modelling errors, uncertainties and unreasonable assumptions in the condition evaluation of the structure. The general goal of this process is to reconcile the experiment and model, and in doing so to identify and explain the root causes of discrepancy in the data and simulated responses. The calibrated FE model can be used in *Step six* through scenario analysis, parametric studies, or what-if simulations, to assist in identifying root causes of damage, designing effective repair and retrofit, risk analysis and bridge management. While St-Id provides the necessary information to the decision-making process, decision-making requires additional considerations and tools. Further, it is important to recognize that St-Id remains an art and its value depends greatly on the talent, heuristics and insight of the coordinator of the entirety of the 6-Steps and those implementing these steps.

Without considering the significance of uncertainty in modelling the bridge system, typical approaches to modelling structures consistently fail to simulate critical behaviours of the system [4], and studies have shown the importance of using experimental data to guide numerical models to improve the reliability of simulations and minimize the discrepancy between the predicted and measured responses of a constructed system [5–7]. In the past decade, St-Id has been applied in the analysis of different types of bridges [8–14], and these research-through-application experiences revealed that one of the most significant barriers to reliable St-Id is associated with errors from inaccurate or

incomplete A-Priori models and model calibration. Many different FE representations of a bridge are possible at various resolutions, and unless the dimensionality, boundary and continuity conditions are realistically represented, the resulting model may appear converged but may not be a reliable digital-twin. For this reason, the heuristics in observing and modelling bridge behaviour is critical for success.

## 2 Finite element model updating

Finite element model updating has emerged in the 1990s as an important area for optimizing the design, construction and maintenance of civil engineering as well as mechanical structures [15]. Calibrating or updating the preliminary model with experimental results is a critical step in the structural identification process, and the use of the experimental data to verify and validate a model eliminates some of the uncertainties and discrepancies regarding how the model simulates the characteristics of the actual structural system [16]. The model updating methods can be generally grouped into two categories: direct updating, and iterative methods. Direct updating consists of correcting the individual terms of the global mass and stiffness matrices until the measured behaviours may be represented [17]. The main disadvantage of direct methods is that directly changing mass and stiffness matrices can lead to the loss of the original physics and geometric connectivity. Because of this shortcoming, the use of direct methods has largely faded. Iterative methods manually or automatically update model parameters in an iterative manner consistent with physics and geometry until the discrepancies between model and experimental responses are reduced to an acceptable level.

Different optimization methods were leveraged to identify parameters that minimize the difference between the measured and predicted data. In most cases, a gradient-based optimization strategy is used. Both linear and nonlinear optimization algorithms, such as thrust-region-reflective algorithm and genetic algorithms, have been implemented to automatically update the parameters [18–20]. For nonlinear analysis, more specific methods such as response surface modelling, particle swarm optimization, Monte Carlo optimization, and genetic algorithms can be used. Recently, finite element model updating has been conducted using Bayesian statistics which gives a probabilistic interpretation of the model parameters [21–30].

Modal analysis outcomes such as natural frequencies and mode shapes extracted from vibration test data can be used as a diagnostic parameter in structural assessment procedures. Over the past decades, modal analysis has gained interest for various types of structures (e.g., single or multiple degree of freedom systems), especially for civil infrastructures which are exposed to dynamic loads [31–34].



Mottershead and Frizwell conducted a comprehensive literature survey of finite element model updating in 1993 [16], which has been used extensively for structural identification. Following that, more technical literature reviews on structural damage identification methods and model updating methods used for the detection, localization and quantification of structural damage were provided by other researchers [35–38]. Bartoli et al., (2017) updated the posterior probability density function (PDF) of the elastic modulus of historic masonry towers using dynamic experimental data in a Bayesian approach considering uncertainties in finite element modelling and measurement errors [39]. Pepi et al., (2019) calibrated a SAP2000 model of a cable-stayed bridge with natural frequencies and mode shapes obtained from ambient vibration testing leveraging an updating Bayesian procedure [40].

### 3 The test bridge and its performance

The test bridge (see Fig. 1a), is a multi-girder steel stringer bridge built between 1983 and 1984 with 100,000 average daily traffic with 5% trucks. The bridge served as a test specimen for exploring answers to the questions in the introduction. North and Southbound traffic is carried by separate structures each featuring 4 simply supported spans (see Fig. 1b). Superstructures are composed of reinforced concrete decks cast on stay-in-place steel forms, detailed with studs to guarantee composite action with the steel girders. Each span is supported by 8 steel girders, laterally braced by steel truss cross-frames. In addition, the outer girders (Girders #1, #2 and #7, #8) are stiffened by horizontal wind-braces that are parallel to the deck. Wind brace members are steel angles directly welded to the webs of the girders near their lower flanges.

The bridge exhibited many performance concerns some of which were captured in a recent inspection report by a credible professional engineering consultant who assigned a Condition Rating of Fair (5) to the superstructure. The rating was driven by the presence of fatigue cracks in the webs of various steel girders, and the settlements and drifting of the approach slabs due to the erosion of the fill under the slabs. A Satisfactory Rating (7) was assigned to the substructures. Additional critical performance concerns that were not indicated in the inspection report were observed and identified by the writers and participating researchers. Examples of some of the performance concerns are shown in Fig. 2.

The next step of an assessment requires identifying potential risks based on the observed performance concerns. Risk of the disutility of a structure should be considered under four lifecycle performance limit states: utility and functionality, serviceability and durability, safety and failure mode; and finally resilience [41]. The observed (and anticipated)

performance deficiencies are classified in each of the critical performance limit states in Table 1. Each one of these Limit States is associated with corresponding demands with different return periods such as daily; 5–25 years; 75–750 years; and, > 1000 Years, respectively [42].

The performance deficiencies that were noted by the bridge inspectors were only the settling and drifting (Fig. 2d) of the approach slabs which caused a significant bump as traffic entered the bridge, and, the progression of the fatigue cracks that formed at the webs of the outermost steel girders to which wind braces were connected as shown in Fig. 2a. The causes for these performance deficiencies were stipulated—the bridge was not designed properly for drainage, and rainwater seeping through the failed joints gradually washed out and eroded the fill under the approach slabs and abutments. Consequently, the approach slabs settled and drifted away from the bridge as shown in Fig. 2d. Researchers attributed the fatigue cracks to the localized lateral distortions at the girder webs caused by the wind brace elements that were directly welded to the web. Due to significant and coupled vertical and lateral vibrations of the superstructure (discussed further in the following) new fatigue cracks continued to form and propagate. During earlier inspection cycles, inspectors recommended drilling holes and inserting bolts at the ends of these cracks to stop their propagation, but this did not stop new cracks from forming. It is interesting that the presence of fatigue cracks has distracted the inspectors from noting and flagging additional performance concerns such as the shear crack at a pier-cap shown in Fig. 2b. Inspectors and bridge engineers assumed the pier-cap shear crack is just another concrete crack such as observed on the abutments or deck. An experienced structural engineer, however, should be able to distinguish between benign versus dangerous cracks, pointing to a structural failure concern.

There were additional performance concerns that were observed by the researchers but were not referenced in the inspection report: (a) significant vertical vibrations exceeded 20%g under truck traffic; (b) the deck exhibited full-width cracks along the span; (c) a significant shear crack at the cantilever extension of the pier cap supporting the first girder of the Southbound Span 2, as shown in Fig. 2b. Of the 4 pier-cap extensions at each end of the span being studied, as well as at any of the other spans, no other pier-cap exhibited such a crack; (d) joints between the simple spans had failed and water draining through these joints severely corroded the bearings. In addition, the plates guiding the rocker bearings failed since the bearings were trying to move diagonally; and, (d) a natural gas pipe ran under the superstructure while a water trunk line crossed the subgrade within the pier foundations. The gas pipe appeared to be affected by the vibrations of the bridge.

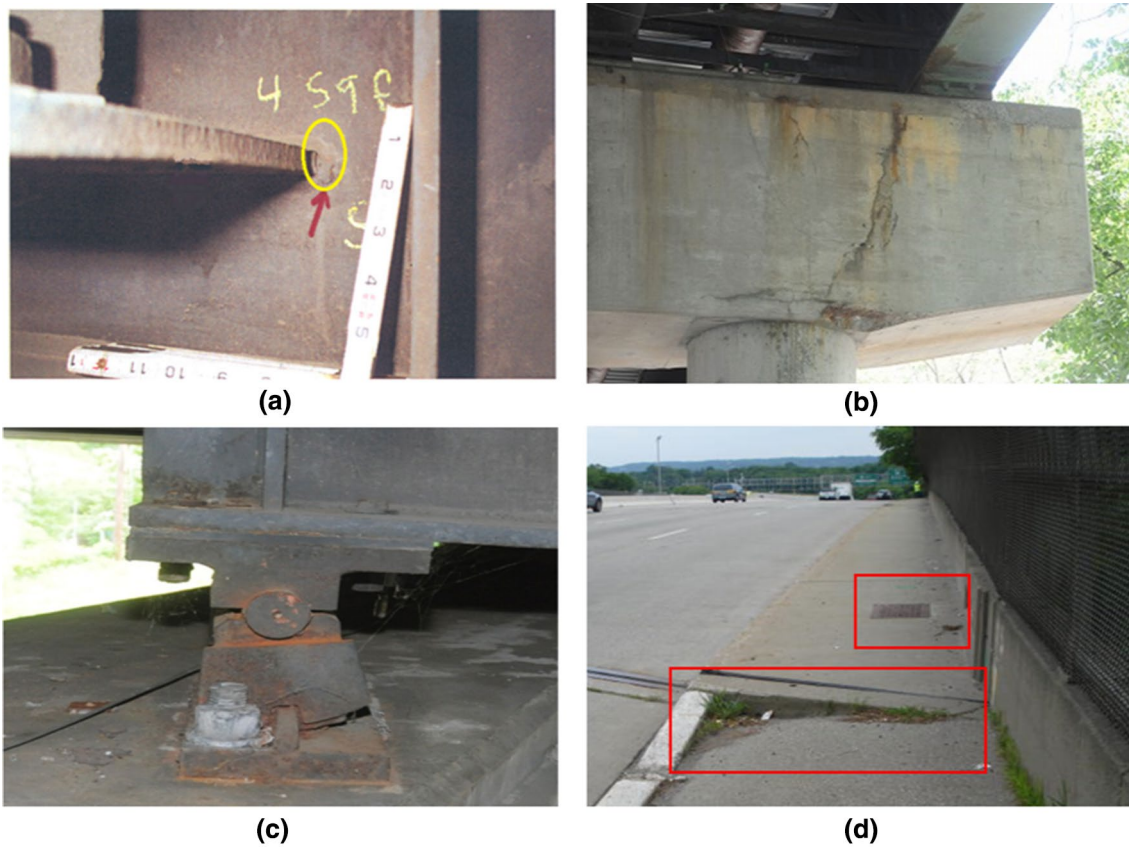


**Fig. 2** Examples of performance concerns: (a) fatigue cracking on girders' web, (b) pier cap cracking, (c) bearing distress, (d) settlement at approaches due to fill erosion

**Table 1** Performance concerns at performance limit states

Functionality	Serviceability/durability	Safety and stability of failure	Resilience
Settlements and bumps at entry due to drifting of the approach slabs	Fill erosion	Fatigue cracks on girder webs	Bridge serves over 100,000 vehicles/day as major link to GWB and to NY City and NE
	Excessive vibrations	Pier cap crack	
	Deck cracking	Gas utility	
	Joint failures		No alternate route
Lack of effective drainage	Bearing corrosion and damage	Trunk-line	Major impacts to regional GDP if the bridge is closed

Whether the Fair (5) condition rating of a 30-Year old bridge on a major artery serving 100,000 vehicles a day—including a substantial truck traffic—and with a multitude of performance deficiencies is acceptable should deserve further discussion. The bridge conditions may have been better characterized with a lesser rating such as (4) indicating the bridge as structurally deficient (mainly due to the pier-cap shear crack) and including it in a retrofit program. While the likely causes of some of the performance deficiencies could be identified by experienced bridge engineers based on heuristics, the causes for the unusual level of vibrations,

deck cracking and especially the single pier-cap shear crack were difficult to explain. A structural identification study explored if simulations could help explaining the causes of these distresses.

#### 4 The experimental program

The experimental program that was carried out by various participants on the Southbound Span 2 is outlined in Table 2. Although some teams focused on the Northbound

**Table 2** The experimental program carried out on the Southbound Span 2

Test Type	Time	Team	Sensors and hardware
Ambient Vibration Testing	April 2010	Drexel University	31 Accelerometers (PCB 393C)
	Sep 2010	Austria (VCE)	BRIMOS kinematic sensors
	July 2010	University at Exeter	Wireless sensors (outer 41 nodes) and wired accelerometers (inner nodes)
	June 2011	Utah State University	20 Sercel L4C 1.0 Hz. Seismometers
	June 2011	KEC & Sejong University, Korea	15 Accelerometers (PCB Model 393B12)
Forced Vibration Testing	June 2011	Drexel University	31 Accelerometers, instrumented hammer, load cell, NI cRIO
	July 2010	University at Exeter	Wireless sensors (outer 41 nodes) and wired accelerometers (inner) + Shakers
Controlled Load Testing	Sep 2010	Drexel University	Strain gages, displacement gages
Laser tracking	Oct 2011	Western Michigan University	Laser tracker, 1.5" and 0.5" reflectors
Long-term Monitoring	2011–2016	Princeton University	Fiber Bragg Grating (FBG) Long Sensors
NDE	June 2011	Rutgers University	IE, ER, HCP, USW, GPR
	June 2011	KCQR & PEC, Korea	Schmidt hammer, UT, GPR

spans, the Southbound Span 2 (Fig. 1b) of the bridge offered greater challenges due to its un-symmetric skew geometry, high vibrations observed and the pier-cap support showing a shear crack.

The ambient vibration testing measured selected displacements, strains and accelerations under traffic and ambient inputs. The forced excitation testing measured accelerations under controlled dynamic input induced by an instrumented impact hammer or by multiple shakers. Controlled load testing measured displacements and strains of the structure under increasing levels of controlled static loads induced by placing loaded trucks at various configurations. Measurements were taken primarily using contact and wired sensors (accelerometers, displacement gages, strain gages) with the exception of an operational vibration test where University of Western Michigan demonstrated the use of laser tracking to measure displacements due to moving traffic.

A fiber optic-based long-term monitoring system was deployed by Princeton University to record strains and temperatures under traffic loads during the period 2011–2016. Finally, wide-area Non-destructive Evaluation (NDE) scans were conducted by Rutgers University to evaluate the condition of the bridge deck, identifying surface and subsurface defects and assessing delamination, concrete modulus and rebar corrosion activity. The Korean team scanned the cracked pier cap by radar to expose the reinforcement or its lack of.

#### 4.1 Vibration testing results

Ambient and Forced Vibration methods have been widely used to extract natural frequencies and mode shapes of bridges and other structures. Ambient vibration refers to the vibration excited by environmental or vehicular inputs.

Ambient vibration testing becomes especially valuable when long-span bridges or other massive structures cannot be excited with conventional excitation techniques such as shakers or controlled impacts. When budgetary constraints preclude the cost of access and traffic control, ambient vibration testing can provide a rapid, relatively inexpensive non-obtrusive method for identifying the modal properties of a structure, in addition to characterizing the response due to the operational inputs. Key aspects include the sensor density, the bandwidth and duration of acceleration measurements and signal processing.

Five different teams used various sensors to collect acceleration data to estimate the natural frequencies and mode shapes during ambient and/or forced vibration testing (Table 2).

The frequencies (within a 15 Hz band) obtained by each team are listed in Table 3. The frequencies obtained by different parties indicated some variations as well as some missed or spurious modes. Modes 1,3,5,8,9,11 were identified as the first six vertical modes of the bridge by leveraging the a-priori model results. Modes 2,4,6,7,10 represented local modes or modes with predominant in-plane motion. Interestingly, some research teams failed to identify the first three flexural modes due to limited instrumentation layouts. The discrepancies were also likely due to different ambient or forced vibration environments, imperfect sensor synchronization, sensor density/modal grid and/or signal processing settings and curve fitting algorithms used by different parties with different hardware and software and at different times. Further, constructed systems may be considerably non-stationary due to how temperature, radiation, wind and humidity may influence the boundary and continuity (bearing) conditions.

**Table 3** Frequencies in Hz. extracted by different groups from vibration tests

Mode	Ambient vibration					Forced excitation	
	Drexel University	Austria (VCE)	KEC & Sejong University	Utah State University	University at exeter	Drexel University	University at Exeter
1	2.89		2.72	2.86		2.98	
2				3.10			
3	3.79	3.75	3.52	3.70	3.75	3.83	3.69
4		4.47		4.50	4.3		
5	5.23		5.14		5.27	5.21	5.22
6			7.75		5.96		
8	9.47	9.18	8.92	9.38	9.50	9.23	9.49
9	11.61	11.79	11.14		11.70	11.74	11.70
10	12.25			12.30	12.40	12.25	12.20
11	14.80	14.81		14.94	14.90	14.80	15.00

The six modes associated with dominant vertical deformations (Modes 1,3,5,8,9,11 in Table 3) were used in finite element model updating as described in the next section. The results obtained by Drexel University were selected for further analysis.

The mode shapes of the Six vertical modes extracted via forced vibration testing by Drexel University are shown in Fig. 3. It is noteworthy that the straight-skew plan geometry

of the span, as well as its mass and stiffness characteristics, led to an unusual “flapping” shape for the first two modes shown in Fig. 3. The straight-skew plan geometry of the span led to significant vibrations with amplitudes of 20%g under ambient traffic conditions (Fig. 4a). A broad spectrum of ambient conditions and traffic input of Span 2SB was extracted from datasets collected during various times of a day (30 min in total). The averaged Power Spectral

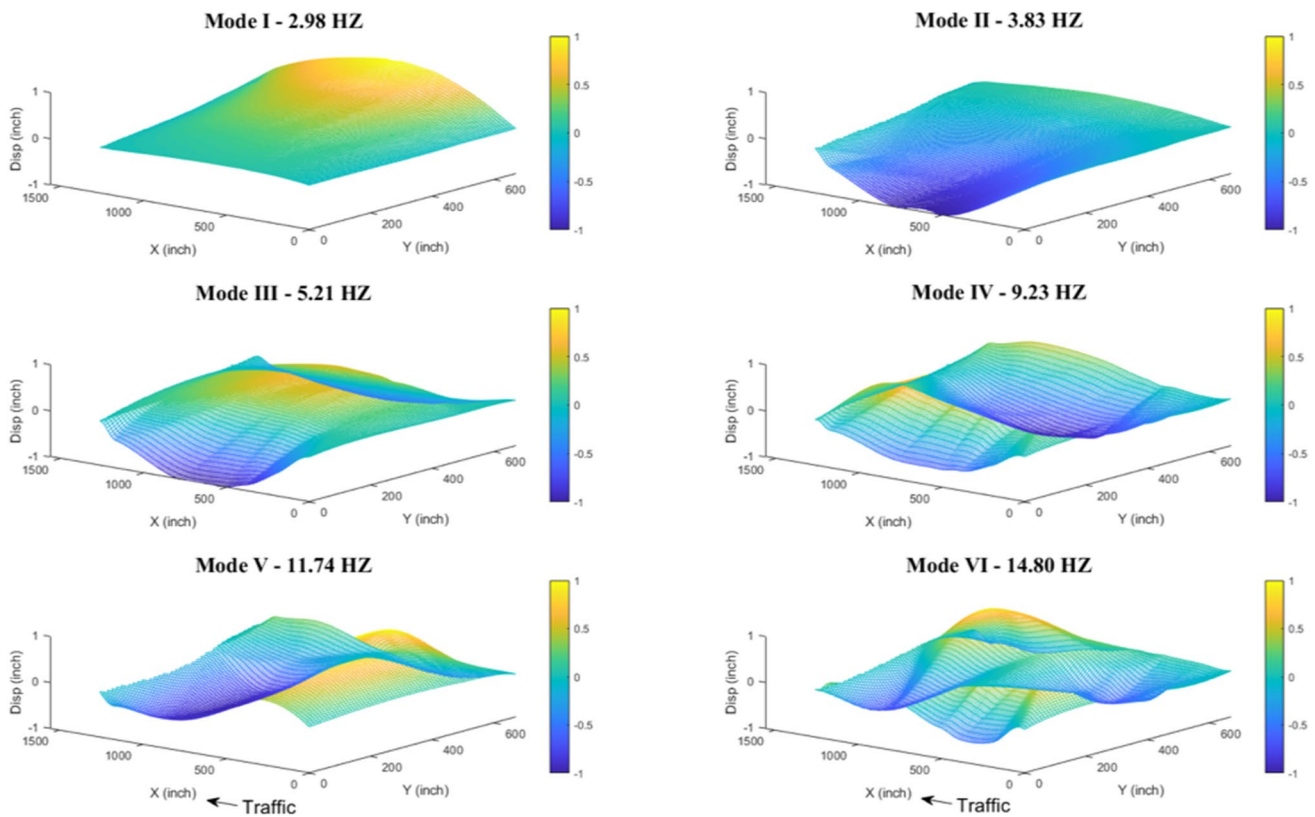


**Fig. 3** Mode shapes from forced vibration testing by Drexel University



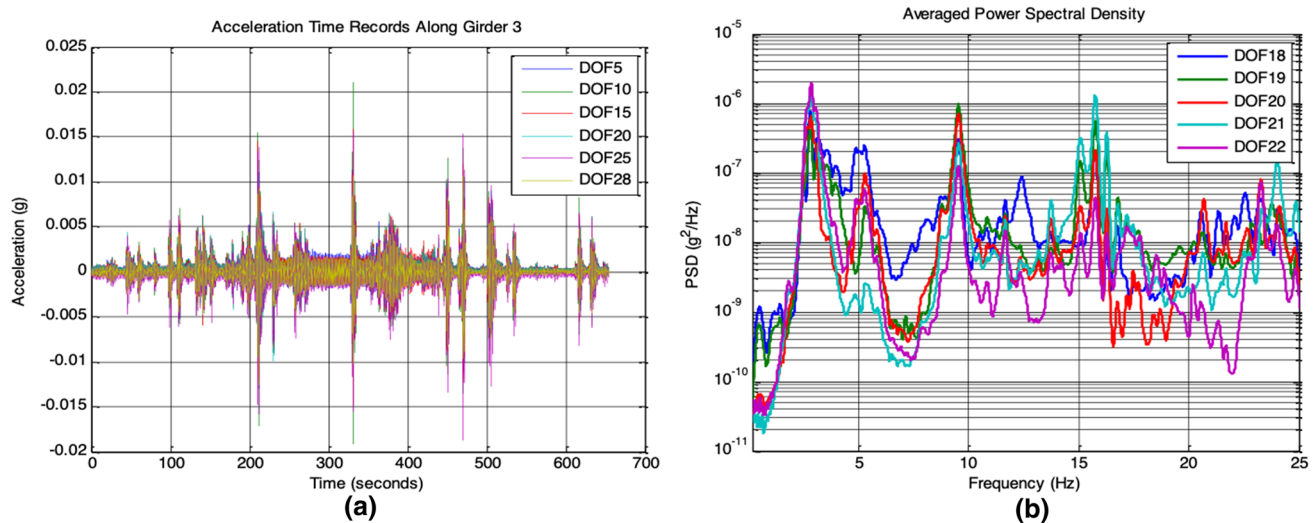


**Fig. 4** Results of ambient vibration monitoring of Span 2SB: (a) vertical acceleration time records of Girder #3; (b) averaged power spectral densities of accelerations at midspan

densities at mid-span are shown in Fig. 4b. As observed from the figure, the input from ambient excitation provided significant energy in the 2–15 Hz Band. This vibration was hypothesized as the principal cause of deck cracking and delamination.

## 4.2 Controlled load testing

Load testing for understanding the safe capacity of a bridge is costly and disruptive. The actual cost often depends on the experience and resources that are dedicated: (a) constraints regarding traffic control; (b) the number and configuration of the trucks used in the loading, the loading program, as well as how loads are positioned on the span; (c) instrumentation selection and grid design; (d) software for real-time visual feedback of bridge responses as different levels of loads are positioned on the bridge. Depending on (a)–(e) it is possible to perform high-speed, crawl or static testing by loaded trucks. In the research program, Dr. Jeff Weidner under Dr. Franklin Moon’s mentorship designed, prepared and executed the load test.

The instrumentation plan is shown in Fig. 5. The primary sensors were clustered into a grid of twelve locations. At each location, a vertical displacement response was collected, as well as two strain responses (strain gages mounted on the top-side of the bottom flange and on the web as shown in Fig. 5b) to allow the extraction of strain profile and the evaluation of the composite action. In a few locations, a third strain gage was added to confirm the linearity of the strain profile.

For the controlled load testing, two lanes were closed to traffic, with complete closure of all lanes when required by the load case. Loads were applied at the mid-span of the closure area with three load stage levels: 3 empty trucks (87

Kips); 3 fully loaded trucks (230 Kips) and 6 fully loaded trucks (460 Kips). The displacement results obtained from the controlled load testing are shown in Fig. 6.

A review of the displacement profiles (Fig. 6a) of Girders #1, #3, #6 and #8 obtained under the full load level indicates that Girder #3 deflects the most at mid-span. This is expected given the static load distribution. A maximum displacement slightly larger than 0.8 inches was measured, corresponding to a drift of  $L/2000$  and implying that the span was 2.5 times stiffer than anticipated by the code ( $L/800$ ). The load–displacement relations (Fig. 6b) also confirm this. However, we also note that at full load, the left end displacement of Girder #1 was as large as that of Girder #3. This was attributed to the cracked pier-cap which allowed an additional vertical deformation of Girder #1 at its bearing. The pier-cap crack-width change was measured during the static test and the crack-width was observed to grow proportionally to the load. The strain profile (Fig. 7) at midspan of Girder #3 indicated linear response (proportionality of strain vs load) with  $\sim 5.40$  Ksi incremental steel stress under full load. However, Girders #8 strain reduced at higher loads—indicating some mechanism causing nonlinearity as load was increased.

The controlled-load testing proved to be the most expensive and disruptive experiment, lasting for 6 h and restricting traffic to only one lane during most of the process, and for this reason the test had to be conducted after midnight. However, the wealth of information and conceptual understanding from the proof-level load displacements and strains made this a most valuable experiment. In fact, in addition to understanding the incremental stress levels under proof level load, it was possible to measure the actual flexibility and capture the nonlinear behaviour which was caused by the pier-cap crack. Although many

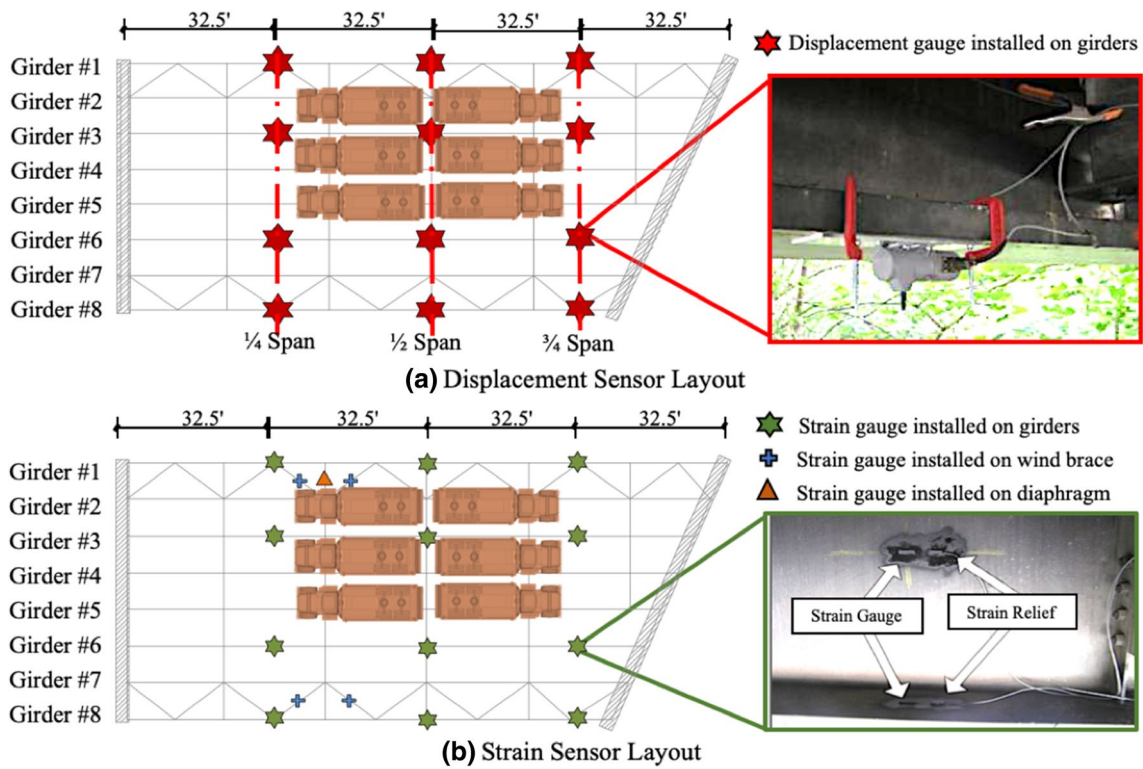
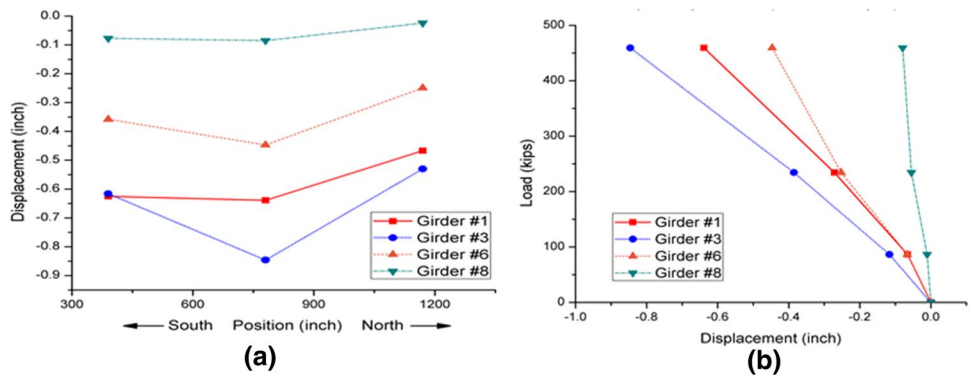


Fig. 5 Instrumentation layout: (a) displacement sensor layout; (b) strain sensor layout

Fig. 6 Controlled static load testing results: (a) girder displacement profiles caused by 6 fully loaded trucks as shown in Fig. 5; (b) midspan load–displacement relations under three loading scenarios (87, 230, 460 Kips)



load test applications rely only on strain measurements, the value of displacement measurements in a load test was observed to be greater, as discussed in the following in relation to parameter identification. Further, displacements are easier to conceptualize and directly relate to any anomalies in structural system behaviour.

### 4.3 Non-destructive testing

The non-destructive testing (NDT) of the deck was performed by Rutgers University. A Korean team of researchers applied NDT to check the rebar details within the

pier-cap at the crack location. The Rutgers team focused on assessing the bridge deck deterioration using six NDE methods, while the Korean team explored the material properties, dimensions, and internal defects, in the vicinity of the crack in the pier-cap.

Concrete bridge decks may go through different stages of deterioration. In many cases, salting agents can penetrate the concrete and cause rebar corrosion, which then results in micro and macro cracking (vertical cracks and delamination), and ultimately produces spalling of concrete. Therefore, the multi-faceted NDT survey of the bridge deck by Rutgers University concentrated on the detection and

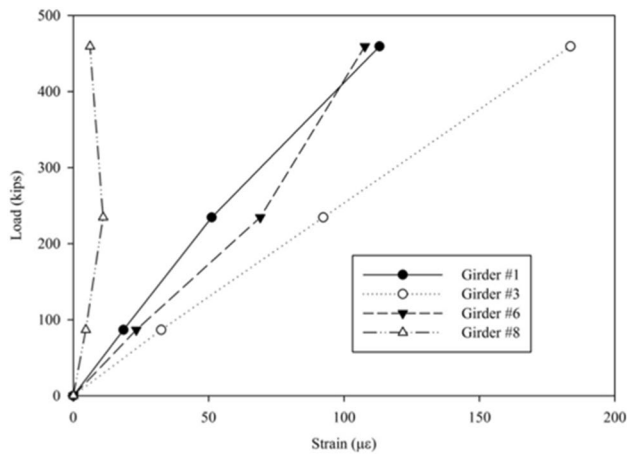


**Fig. 7** Mid-span strains from the strain gages at the bottom flange for the three load scenarios applied at the center

characterization of three deterioration types: corrosion, concrete degradation, and delamination.

The Impact echo method was used to detect and characterize delamination, the electrical resistivity to assess corrosive environment, half-cell potential to determine the probability of active corrosion, ultrasonic surface waves method to estimate concrete modulus, ground-penetrating radar to measure concrete cover and provide a qualitative

deterioration assessment, and microwave technology by MoistScan detected areas of higher moisture content. The survey was conducted by discretizing the deck into a 0.61 m (2 ft) by 0.61 m (2 ft) grid. The first survey line (the longer side shown in Figs. 8, 9, 10) was one foot away from the curb, and the scanned area covered the first two lanes of Span 1SB and Span 2SB. Some of the NDT results of Span 2SB, the area of which is 6.0 m (20ft) by 40.0 m (130ft), are shown in Figs. 8, 9, 10, and the results of the survey corresponding to delamination and corrosion are discussed further in the following.

Results of the Ultrasonic Surface Wave measurements, shown in Fig. 8 point to a low concrete strength, considering that the measured modulus was mostly in a 13,800 to 27,500 MPa (2000–4000 ksi) range. This was confirmed through the review of design plans, which specified a low concrete modulus for the deck. The impact echo test results shown in Fig. 9 point to significant delamination in the deck. This was somewhat surprising, considering the low corrosion activity measured by Half-Cell Potential (Fig. 10) and fair corrosive environment obtained from Electrical Resistivity. Given that the extent of delamination could not be caused by corrosion of reinforcement, the NDT scans further implied large vibrations as a possible reason for the widespread delamination.

**Fig. 8** Results from ultrasonic surface wave testing showing concrete estimated modulus for Span 2 SB

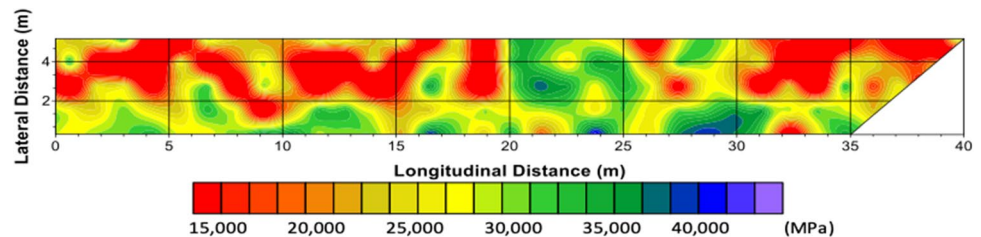


**Fig. 9** Results from impact echo testing showing delaminations for Span 2 SB

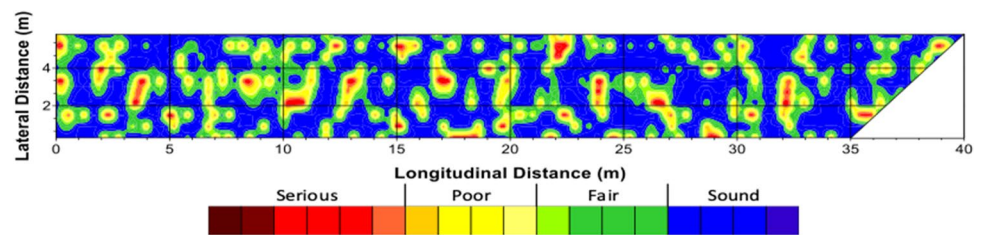
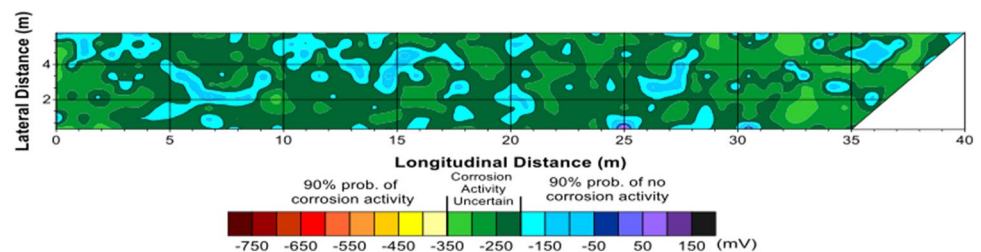


**Fig. 10** Half cell potential testing results showing probability of corrosion activity for Span 2 SB





The NDT scan by the Korean team included the measurement of concrete strength of abutments and piers by Schmidt Hammer test, the measurement of crack depth using a concrete ultrasonic tester, the detection of rebars in the abutment and pier structures by Reinforced Concrete (RC) radar (see Fig. 11a), the measurement of paint thickness of steel girders using a digital coating thickness gauge, the measurement of the thickness of steel members and the detection of internal defects in welded areas with an ultrasonic tester. One noteworthy finding was the poor arrangement of rebars in the pier-cap crack location. In the cracked area of the north-bound abutment of the bridge (see Fig. 1b), the measured spacing of horizontal rebars (= 43 cm) is larger than the recommended design spacing (= 30 cm). In addition, in the cracked pier cap (see Figs. 2b and 11a), there was no vertical rebar (see Fig. 11b) within a distance of 1 m around the detected vertical crack.

**4.4 Long-term monitoring by fiber-optic sensors**

Princeton University researchers instrumented six cross-sections of Girders #2 and #5 along their top and bottom flanges by long-gauge FBG sensors in parallel topology (12 strain sensors and 12 temperature sensors).

Analysis of data after 1-Year of monitoring (Fig. 12b, c) revealed that the neutral axis locations along the length of the girders remained stable except at the left end of Girder #2. The neutral axis locations shifted (shown on the top left of Fig. 12c) in the course of the year, implying a progression of delamination of the deck in the vicinity of the cracked pier cap and indicating a possible loss of composite action at this region.

**5 Finite element model updating**

Two finite element models were developed with Abaqus [43] for the test bridge. The a-priori model (Fig. 13) was developed and based on the design drawings, and parameters were adjusted to account for the actual condition of the critical bridge components observed during the visual inspection. The close-up details of the model, showing how the girder, deck, pier and the bearings are represented, are illustrated in Figs. 13 and 14. The bridge deck, as well as the webs, flanges and stiffeners of the steel girders, were modeled using 8-node 3D shell elements. Wind-bracings and cross frames, which connect the girders, were modeled using 3-node quadratic 3D beam elements (Timoshenko beams). The parapet and barrier were modeled as beam elements

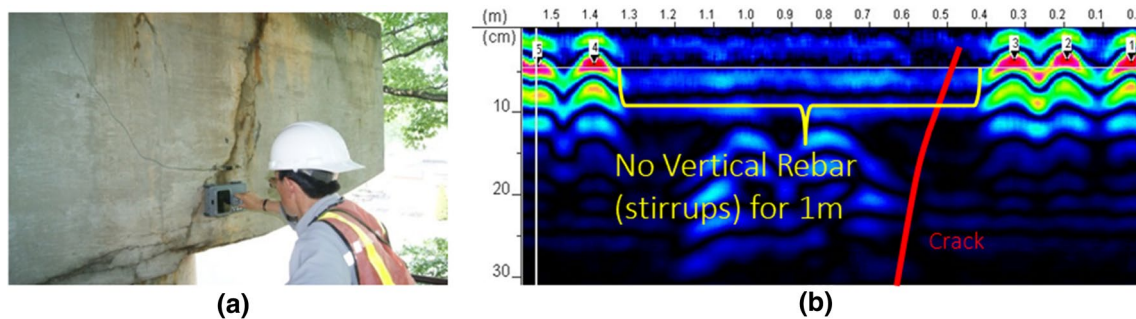


Fig. 11 Application of RC radar and corresponding results in cracked pier cap

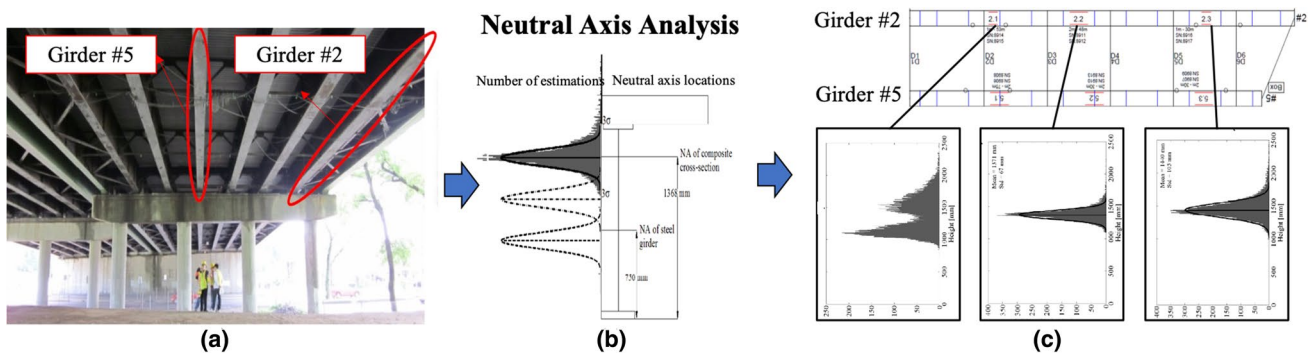
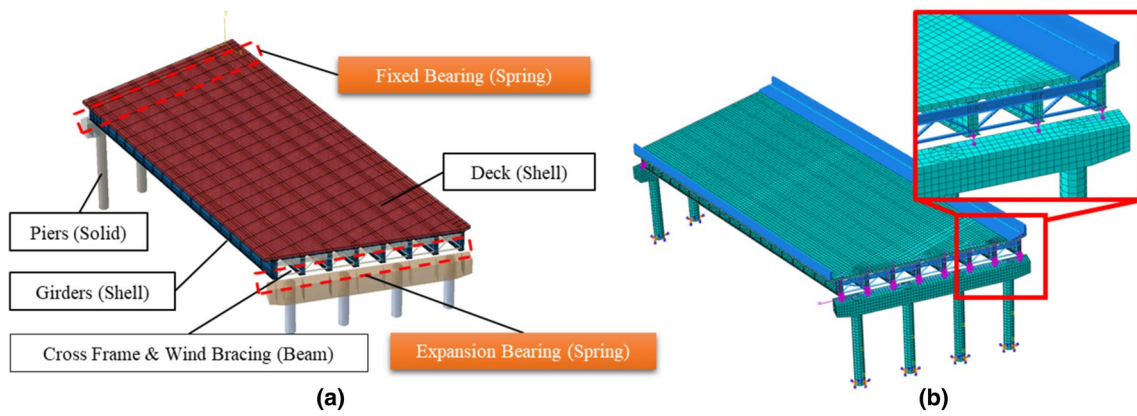


Fig. 12 Long-Term monitoring analysis: (a) site view of the bridge with instrumented girders #2 and #5 marked; (b) neutral axis analysis of strain data; (c) 1-year results from neutral axis analysis





**Fig. 13** Finite element model (with Piers) using Abaqus: (a) Nomenclature; (b) Meshing

connected to the deck using rigid links. The steel girders were connected to the deck by shear connectors modeled using beam elements with a high value of the elastic modulus for the baseline modeling representing fully composite action.

The material properties of steel for girders, cross frames and bracings complied with the specifications of ASTM(S) A36 according to the design drawings. Bridge piers were modeled with 3D solid elements. A mesh size of 6 in. was chosen for all the parts of the model after a mesh size convergence analysis, and the meshed model is shown in Fig. 13b. To simulate the dynamic properties of the bridge such as frequencies and mode shapes, the entire FE model was analyzed as the inertia properties of the substructures significantly impact the frequencies of the system. In simulating the static properties of the system, only a free-body-diagram of the superstructure was analyzed.

The south supports of span 2 SB are fixed bearings, and the north supports are rotating (rocking) movable bearings (see Figs. 13a and 14b). The boundary conditions at each bearing were represented by spring elements acting in 3 directions:  $K1\_L$  and  $K1\_R$  are spring stiffnesses along with

the longitudinal directions of fixed bearings and expansion bearings;  $K2\_L$  and  $K2\_R$  are vertical spring stiffnesses, and  $K3\_L$  and  $K3\_R$  refer to springs acting along the lateral direction). The shear connectors between deck and girder were modeled as beam elements, and Young’s modulus of the shear connector ( $E\_shear\_connector$  shown in Fig. 14a) was selected as one parameter for model updating.

To calibrate the a-priori model, experimental data obtained from vibration tests and static truck-load tests were processed and interpreted for model updating. The NDE test results were used to define the bounds for material properties in the FE model. The initial values of the parameters listed in Table 4 were used as starting points for the optimization.

The a priori model was both manually and automatically calibrated by considering the experimental data. Manual calibration consisted of adjusting parameter values based on their expected influence on model characteristics and responses. The goal of this approach was to identify a set or parameter values which adequately represented the experimental behaviour. Although labour intensive, this process allows the user to explore the parameter space

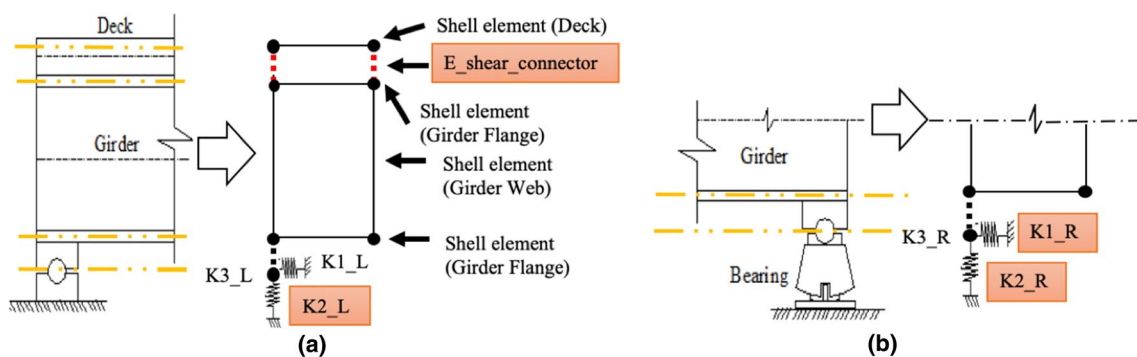


**Fig. 14** Model details of bridge bearings: (a) South fixed bearings; (b) North expansion bearings; L and R stand for Left (South) and Right (North); 1, 2 and 3 stand for longitudinal, vertical and lateral directions

**Table 4** Initial values assumed for the critical parameters of the FE model

Parameters	Description	Initial Value
D_Deck	Density of deck	0.086 lb/in <sup>3</sup>
E_Deck	Young's modulus of deck	3453 ksi
E_Parapet	Young's modulus of parapet	3453 ksi
K2_L, K2_R	Vertical bearing stiffness at Left and right side	500 k/in
K2_L1	Vertical pin bearing stiffness above pier-cap (along South Side)	500 k/in
K3_R	Lateral rocker bearing stiffness (along North Side)	500 k/in
E_shear_connector	Young's modulus of shear connectors (measure of composite action)	3 × 10 <sup>4</sup> ksi

with more freedom and helps the development of heuristics and intuition about the bridge's characteristics.

The Abaqus Scripting Interface, a customized extension of standard Python, was used to modify parameters in the Abaqus models and to obtain static and dynamic responses from the models. The automated calibration utilized the Matlab optimization function *fminsearch* [44], (which is based on the Nelder-Mead simplex algorithm) to minimize the objective function of interest. Parameter limits were included in the Python scripts to bound the search region of the *fminsearch* function which is an unconstrained multivariable function. To mitigate the influence of local minima, multiple iterations of the automated calibration were performed using different sets of initial parameters.

### 5.1 Model updating with vibration testing data

Parameter identification was performed using the first six modes (modes 1, 3, 5, 8, 9, 11 shown in Table 3) and first four modes (modes 1, 3, 5, 8 in Table 3) derived from ambient and forced vibration testing conducted by Drexel University. Modes derived from numerical models may include local modes of members, therefore, finding the corresponding modes for the modes extracted experimentally is a critical step in the automated updating process. In this study, the Modal Assurance Criterion (MAC) of the mode shapes, a statistical indicator that is sensitive to the largest difference between comparative values and insensitive to small changes or small magnitudes, was used in conjunction with a frequency comparison to pair experimentally and numerically extracted modes. The MAC value is defined as:

$$\text{MAC}_{ij} = \frac{|\phi_{a_i}^T \phi_{e_j}|^2}{\phi_{a_i}^T \phi_{a_i} \phi_{e_j}^T \phi_{e_j}} \quad (1)$$

where  $\phi_{a_i}$  is the  $i$ -th mode shape of the numerical model;  $\phi_{e_j}$  is the  $j$ -th mode shape of the test bridge,  $\phi_{a_i}^T$ ,  $\phi_{e_j}^T$  are the transpose of the mode shapes,  $\text{MAC}_{ij}$  is the MAC value for the

$ij$ -th mode pair. The MAC is bounded between 0 and 1, with 1 indicating fully consistent mode shapes and 0 indicating that the modes are not consistent.

Corresponding numerical mode shapes of a sought experimental mode can be identified by finding the max MAC value for the modes within a frequency range (i.e.  $\pm 5$  Hz around the mode frequency). Local modes and modes with predominant in plane motion can occasionally provide large MAC values and thus, it will be helpful to filter out such numerical modes before the comparison with the experimental mode shapes. For instance, a simple filtering method was proposed to remove lateral modes by limiting the maximum longitudinal displacement to 30% of the maximum vertical displacement and the maximum lateral displacement to less than 50% of the maximum vertical displacement.

When both natural frequencies and mode shapes were leveraged, the objective function implemented for model updating was defined as:

$$f = \frac{1}{n} w_{f_i} \sqrt{\sum_{i=1}^n (f_{e_i} - f_{a_i})^2} + \frac{1}{n} \sum_{i=1}^n w_{m_i} \left( \frac{1 - \sqrt{\text{MAC}_{ii}}}{\sqrt{\text{MAC}_{ii}}} \right) \quad (2)$$

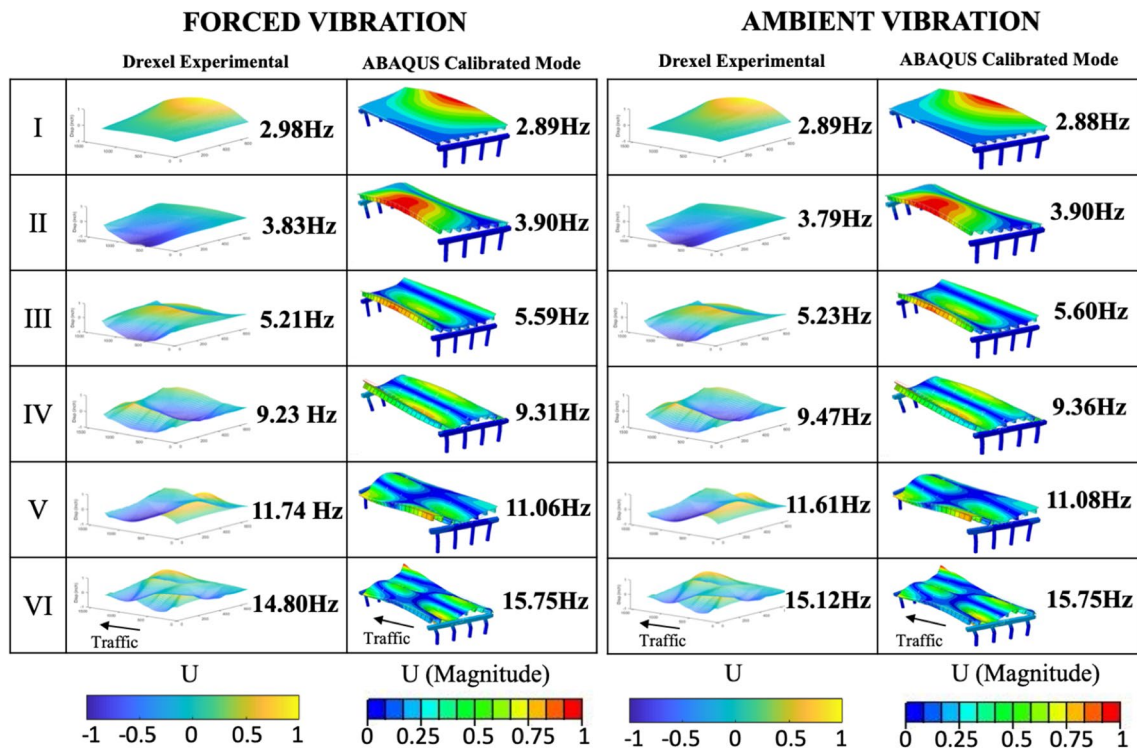
where  $w_{f_i}$ ,  $w_{m_i}$  are weighting factors (assumed as  $w_{f_i}=10$ ,  $w_{m_i}=1.0$ ),  $f_{e_i}$  is the  $i$ -th modal frequency of the test bridge,  $f_{a_i}$  is the  $i$ -th modal frequency of the FE Model,  $\text{MAC}_{ii}$  is the MAC value for the  $i$ -th mode pair,  $n$  is the number of modes.

Table 5 presents the parameter values corresponding to the updated models (calibrated with ambient and forced vibration data), while the frequencies and corresponding mode shapes are shown in Fig. 15. As shown in Table 5, the updated value of K2\_L1, the vertical stiffness of the spring representing the South Support Stiffness under Girder #1 (i.e. stiffness provided by the cracked pier-cap), is significantly decreased using the first 4 or 6 modes of ambient vibration data and the first 6 modes of forced vibration data. All other parameters remain fairly uniform irrespective of the experimental dataset used for calibration.

The results in Fig. 15 imply that if Operational Monitoring (a strategy significantly cheaper and non-disruptive compared to a MIMO modal analysis) is carefully executed, even

**Table 5** Values of critical parameters updated using vibration testing datasets

Parameter	Units	Initial model	Bounds	Calibrated with ambient vibration data		Calibrated with forced vibration data	
				First 4 modes	First 6 modes	First 4 modes	First 6 modes
D_Deck	lb/in <sup>3</sup>	0.086	[0.07,0.1]	0.085	0.085	0.085	0.085
E_Deck	ksi	3453	[3000,4500]	3733	3733	3733	3555
E_Parapet	ksi	3453	[3000,4500]	3555	3555	3555	3733
K2_L, K2_R	k/in	500	[0,1000]	350	350	350	350
K2_L1	k/in	500	[0,1000]	100	100	350	100
K3_R	k/in	500	[0,1000]	485	485	485	485
E_shear_connector	ksi	3.0 × 10 <sup>4</sup>	[2.9 × 10 <sup>4</sup> , 10 <sup>10</sup> ]	3.0E05	3.0E05	3.0E05	3.0E05



**Fig. 15** Comparison of experimental and numerical frequencies and modes

if a relatively small number of modes are properly extracted, a digital twin capable of capturing critical structural behavior can be generated. Standards to guarantee the successful implementation of Operational Monitoring in terms of sensors and density, data collection and processing should be collated from a few experts who have refined this method.

It is noteworthy that the first 4 modes of ambient vibration data delivered the same updating results as the first 6 modes of ambient vibration data, as well as appeared sufficient in observing a stiffness decrease at the cracked corbel although a reduction in the number of modes used for parameter updating can affect the estimates of the parameters.

### 5.2 Model updating with controlled load testing data

The displacements and strains obtained from 12 locations (at 1/4, 1/2, 3/4 Span of Girders #1, #3, #6, and #8 shown in Fig. 5) for 6 fully loaded trucks were used for model updating. The automated calibration was executed using both displacement and strain measurands together, as well as considering each response modality independently. The objective functions implemented were defined for the three scenarios as:

Displacement objective function:

$$f = \frac{1}{n} w_d \sqrt{\sum_{i=1}^n (\text{Disp}_{e_i} - \text{Disp}_{a_i})^2} \quad (3)$$

Strain objective function:

$$f = \frac{1}{n} w_s \sqrt{\sum_{i=1}^n (\text{Strain}_{e_i} - \text{Strain}_{a_i})^2} \quad (4)$$

Displacement and Strain objective function:

$$f = \frac{1}{n} w_d \sqrt{\sum_{i=1}^n (\text{Disp}_{e_i} - \text{Disp}_{a_i})^2} + \frac{1}{n} w_s \sqrt{\sum_{i=1}^n (\text{Strain}_{e_i} - \text{Strain}_{a_i})^2} \quad (5)$$

where  $w_d$ ,  $w_s$  are weighting factors (assumed equal to 1.0) for displacement and strain,  $\text{Disp}_{e_i}$ ,  $\text{Strain}_{e_i}$  are the experimental displacement and strain at the  $i$ -th location,  $\text{Disp}_{a_i}$ ,  $\text{Strain}_{a_i}$  are the displacement and strain obtained from the Abaqus model at the  $i$ -th location.

Table 6 presents the experimental results and calibrated analytical results using displacement and strain measurements for model optimization. First, only the displacements were considered in the calibration using Eq. 3. Then only the strains were considered (Eq. 4). Finally, the Objective Function in Eq. 5 that incorporates both displacements and strains was used.

Calibration using only displacement data and both displacement and strain data resulted in similar values for the parameters of the final calibrated model. Calibration using only strain data did not identify the same parameter values resulting in a smaller reduction for the stiffness of the cracked pier cap (K2\_L1). This is attributed to the fact that strain responses were highly localized and were not as significantly affected by the selected model parameters as the displacements. Further, strain signal to noise values were much smaller than displacements and therefore were influenced much more by noise and numerical computational errors.

The vertical displacements of Girders #1, #3, #6, and #8 obtained from the manually calibrated model (with displacement data) is compared with the displacements measured during controlled load testing (Fig. 16a). A

discrepancy in the vertical displacement at 1/4 span (the node located at 390 inches from the south support) of Girder #1 remained even after calibration. This suggests that the linear model is unable to accurately simulate the cracked pier-cap's lack of stiffness even after optimization. The actual impacts of the pier-cap crack onto the serviceability, durability and safety of the bridge is paramount. Due to the structural damage of the pier-cap, the superstructure ends up transferring the loads to other bearings that are properly supported by the undamaged middle region of the pier. The continued degradation of the deck as well as the possible loss of composite action in the vicinity of the cracked pier which were indicated by the long-term monitoring by Princeton researchers corroborate this observation.

To address the discrepancy, an additional parameter E\_shear\_connector\_L1 (Young's modulus of shear connectors of 1/3 span of Girder #1 and #2), was added for automated calibration. The initial value of the new set of parameters is shown in Table 7.

Table 7 summarizes the parameter optimization results obtained by leveraging both the displacements and strains measured during the truckload test under full load. The simulated displacement profiles of the instrumented girders well-correlate with the experimental measurements except for Girder 1 in Fig. 16b.

The values of measured versus simulated displacements and strains are compared in Table 8. As the measured displacement or strain becomes small, the percentage error between measured and simulated responses increase given the nature of the objective function which prioritizes larger measurement values (which have a larger experimental signal to noise ratio). In general, displacement discrepancies of 15% and strain discrepancies of 25% are noted if we ignore the errors for the extremely low strain responses close to the measurement systems' sensitivity threshold.

An observation is that in spite of the nonlinearity (due to deck cracking and delamination as well as the shear crack in one pier-cap), it was possible to calibrate a finite-element model with parameter calibration errors remaining within

**Table 6** Values of manual parameters updating using controlled load testing datasets

Parameter	Units	Initial model	Bounds	Calibrated with displacement	Calibrated with strain	Calibrated with displacement and strain
E_Deck	ksi	3453	[2000,4500]	3733	3733	3733
E_Parapet	ksi	3453	[2000,4500]	3750	3555	3750
K2_L, K2_R	k/in	500	[0,1E04]	920	829	920
K2_L1	k/in	500	[0,1E04]	200	350	200
K3_R	k/in	500	[0,1E04]	500	485	500
E_shear_connector	ksi	3.0E04	[0,1E07]	3.0E06	3.0E04	3.0E06



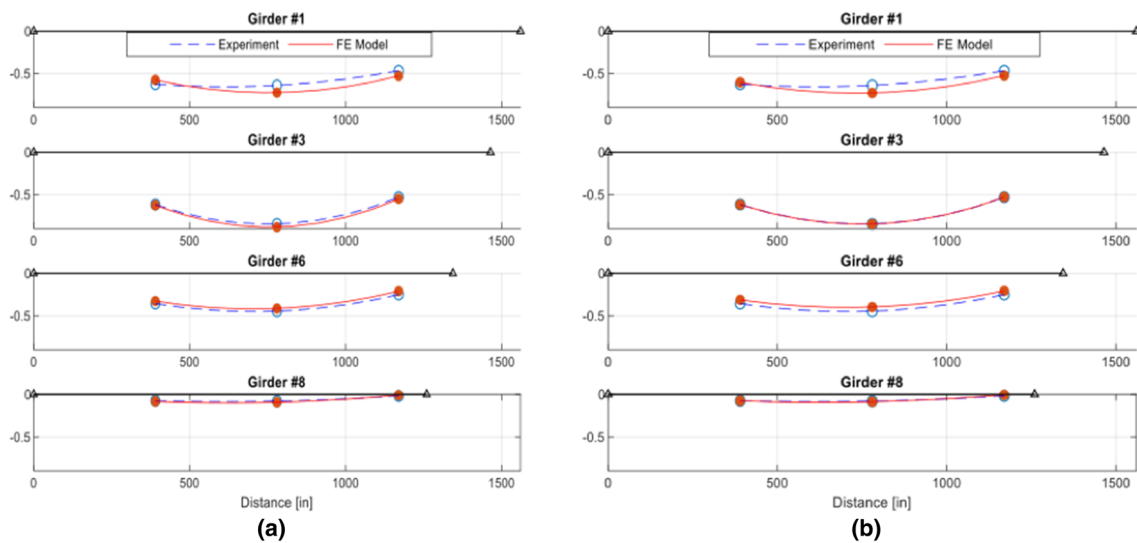


**Fig. 16** Vertical displacements comparison: (a) results obtained from manually calibrated model with initial parameters; (b) results obtained from automatically calibrated model with new start point

**Table 7** Values of automated parameters updating using controlled load testing datasets

Parameter	Units	Initial model (new starting point)	Bounds	Calibrated with displacement	Calibrated with Strain	Calibrated with displacement and strain
E_Deck	ksi	3453	[2000,4500]	4500	4500	4500
E_Parapet	ksi	3453	[2000,4500]	4500	4500	4500
K2_L, K2_R	k/in	500	[0,1E04]	1275.33	9685.12	1303.93
K2_L1	k/in	0.1	[0,1E04]	0.0	0.0	0.0
K3_R	k/in	500	[0,1E04]	92.95	575.78	106.82
E_shear_connector	ksi	3.0E06	[0,1E07]	6.77E06	9.84E06	4.25E06
E_shear_connector_L1	ksi	0.1	[0,1E07]	0.12	0.0	0.10

**Table 8** Summary of model updating leveraging static testing

Location	Measured Disp. (in)	Simulated model Disp. (in)	Diff (%)	Measured strain	Simulated model strain	Diff (%)
Girder 1—1/4	-0.625	-0.603	3.47	8.60E-05	8.60E-05	0.32
Girder 3—1/4	-0.616	-0.617	-0.22	1.12E-04	1.35E-04	-20.66
Girder 6—1/4	-0.358	-0.312	12.86	7.70E-05	7.70E-05	1.09
Girder 8—1/4	-0.075	-0.075	0.00	1.60E-05	3.60E-05	-131.51
Girder 1—2/4	-0.639	-0.728	-13.98	1.13E-04	1.22E-04	-7.86
Girder 3—2/4	-0.846	-0.847	-0.07	1.84E-04	2.36E-04	-28.55
Girder 6—2/4	-0.447	-0.398	10.92	1.08E-04	1.19E-04	-10.05
Girder 8—1/4	-0.079	-0.086	-8.30	6.00E-06	3.00E-05	-383.60
Girder 1—3/4	-0.467	-0.525	-12.37	8.40E-05	1.03E-04	-22.93
Girder 3—3/4	-0.53	-0.528	0.33	1.18E-04	1.24E-04	-4.75
Girder 6—3/4	-0.249	-0.205	17.65	7.00E-05	6.90E-05	1.58
Girder 8—3/4	-0.019	-0.006	70.22	5.00E-06	1.90E-05	-273.20

5% for the frequencies, 15% for girder displacements and 25% for girder strains that exceed sensor sensitivity.

While the finite-element model does point to a damage at a location corresponding to the pier-cap crack, it does not directly indicate the severity of the damage given its resolution. To increase such resolution, individual shear studs representing composite action could be considered as independent variables to update. However, this would have resulted in too many parameters to update causing other uncertainties in the optimization process. A digital twin (high-resolution FE model) of the structure could also incorporate the NDE scan results to account for the local distribution of delamination as well as estimated concrete stiffnesses.

Updating a digital twin proved to be a complex process. Difficulties including convergence to local minima of the objective function can lead to unreasonable parameter identification. The variability of the parameter values obtained using ambient and forced vibration as well as displacement and strain information confirm such challenges, as shown in Tables 5, 6 and 7. Some parameters have limited influence on the measured static and dynamic deformation of the bridge and their identification prove challenging (for instance K3\_R, representing the bearings stiffness along the lateral direction 3). However, parameters which strongly influence the measured static and dynamic deformation of the bridge, such as the spring stiffness K2\_L1 (reaction stiffness of the cracked corbel) consistently converge to quantities lower than initially assumed.

Focusing on this critical parameter, the optimization of the digital twin with static measurements under proof load unequivocally highlighted the corbel deficiency (K2\_L1 ~ 0 in Table 7). The digital twins calibrated with the forced vibration and even the inexpensive ambient vibration testing results point to the same damage mechanism. Operational monitoring or ambient vibration testing, when properly implemented, can successfully identify performance concerns and provide the best benefit/cost value for condition assessment.

### 5.3 Scenario simulations

As previously mentioned, the pier-cap at the south end of Girder #1 was the only cracked pier-cap for the entire bridge. This could be a consequence of design or construction shortcomings. Recall that the radar test results in the vicinity of the crack pointed to a lack of shear reinforcement (Fig. 11b). However, it is not known if other piers had similar design and construction flaws.

The model calibrated using displacement measurements only was used for several simulations with moving vehicles, and assuming fully composite action and idealized supports (fixed bearing and expansion bearing) in order

to simulate the bridge when it was NEW. The most severe load combination due to three trucks (two trucks moving along Lane 1 and one truck moving along Lane 2) was sought. To accomplish this, cross correlation was computed between the time series of total reaction forces on Bearing 1S and Bearing 1N caused by separate moving loads acting on Lane 1 and Lane 2. Considering a minimum distance (50 ft) between two trucks on the same lane, a load combination of three trucks was adopted as the most severe for both dynamic and static analysis. The simulation results shown in Fig. 17 represented a load scenario maximizing shear stresses at the cross section of the cracked pier-cap.

Numerical values of the maximum shear stresses in the pier cap were summarized in Table 9, and a Dynamic Amplification Factor (DAF) value of 1.28 was calculated by the ratio of dynamic and static live load shear stresses. The maximum shear stress under dead load stress alone is slightly larger than the concrete shear capacity within the pier cap. The maximum shear stress under dead load and dynamic truckloads is 135 psi, exceeding the shear capacity of concrete at the pier-cap (110 psi). Such stresses, in absence of shear reinforcement (see Fig. 11b), are likely responsible for the shear crack at the corbel. Consequently, the South end of Girder 1 virtually lost its support stiffness causing loads to be redistributed to other bearings.

The American Association of States Highway and Transportation (AASHTO) Load and Resistance Factor Design (LRFD) specification [45] indicates the dynamic amplification factor as 1.33 for bridges. The DAF 1.28 obtained from finite element model simulations is very close to the DAF 1.33 defined in the design code. However, the influence of surface roughness, which had been proven to be an important factor for DAF [46–48], was not taken into account in the simulation. To obtain a more reliable dynamic amplification factor under moving truckloads, surface roughness should be experimentally evaluated by profiling the bridge deck and further analysis may be conducted to explore the effects of other parameters [46–54, 55], such as vehicle speed, structure damping properties, vehicle mass, stiffness and damping of suspensions and tires. There is evidence that amplification factors much higher than 1.33 may be possible for responses such as bearing reactions when all of the critical parameters governing actual truck crossing effects on bridges are considered.

## 6 Conclusions

The “International Bridge Study” revealed design, construction and maintenance shortcomings that have led to multiple bridge performance concerns. It was possible to pinpoint the root causes of some of the deteriorations

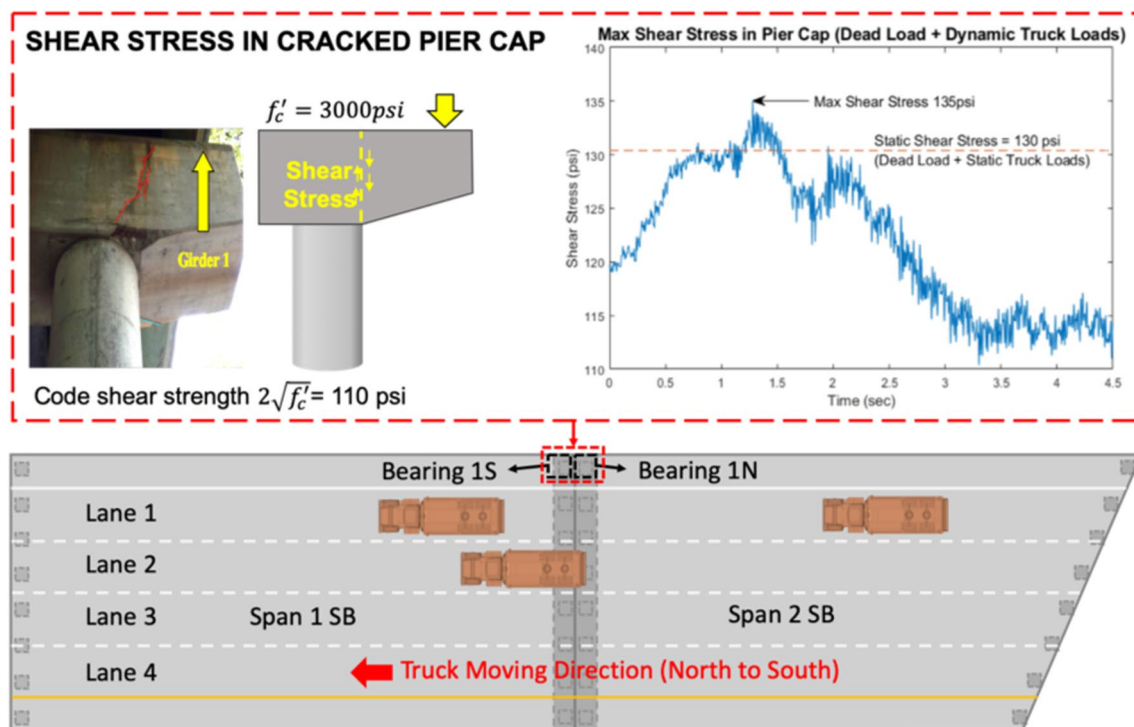


**Fig. 17** Simulation results of three moving vehicles: (top) maximum shear stress estimated in the corbel cross section; (bottom) trucks configuration causing maximum reactions at bearings 1S and 1N supported by cracked corbel

**Table 9** Maximum shear stresses obtained from the simulation of three moving trucks

Actions	Max corbel shear stress and DAF
Dead load	114.0 psi
Static truck load	16.36 psi
Dynamic truck load	21.00 psi
DAF	1.28

and damage by heuristics. For example (a) the settlements of the approach slabs were obviously caused by the erosion of the fill under them due to bridge rainwater not being properly drained; (b) the connection details of the wind-bracing to the main girder webs created lateral distortions at these points, which were aggravated by coupled vertical and lateral vibrations of the bridge and led to fatigue cracking. The lateral braces were observed to cause web fatigue cracking at a number of other bridges and their direct welding on to the web were already identified by FHWA as a fatigue-critical detail. The lateral stiffness provided by these braces could have been better provided by diaphragms; (c) the failures of many rocker bearings were due to the tendency of the bridge movements due to live loads and temperature effects to occur along various directions which were not accommodated

by the single-direction rockers. These bearings need to be replaced by neoprene bearings that have the capacity to move in many lateral directions.

The study also demonstrated that heuristics may not be sufficient for diagnosing and mitigating all of the root causes for the performance deficiencies of the test bridge. For example, the pier-cap shear crack was not even recorded by inspectors. The study, therefore, demonstrated the value of an integrated and scientific approach to condition and performance evaluation by leveraging the structural-identification concept. By designing and interpreting the field experiments supported by proper analytical prediction using the A-Priori model, a greater value was achieved from the field experiments. It was possible to design a load test with real-time monitoring of critical bridge responses. The integration of a sufficient number of sensors such as accelerometers, strain and displacement transducers provided valuable and necessary information for a mechanistic understanding and robust modelling of the bridge for simulations. What is most important, however, is that the conclusions of structural identification for a small sample of bridges may be extended into generic understanding of design errors and inspection shortcomings in the current practice.

Based on the analysis of the field experiments and model updating, the following general conclusions could be formulated:

1. Ambient vibration testing by operational monitoring, if performed and processed properly, successfully revealed the first several modes and frequencies of the structure. These were shown as adequate for parameter identification of a numerical model of the bridge; the much costlier forced vibration test by impact or harmonic inputs did not offer a clear advantage against ambient vibration in terms of information value except that the uncertainty in the test results would be reduced.
2. Controlled proof-load testing was especially useful in demonstrating the location and effects of damage (even when damage may not be visible) and the reserve live-load capacity of the bridge in spite of the damage given that the maximum stress under proof-load level was 5 ksi under 460 Kips of concentrated proof-level truck load. The challenge in designing this kind of testing is to apply the load in increments and monitor and visualize response in real-time for safety. Significant load i.e. six dump trucks fully loaded by road salt were required for this test and the bridge had to be closed to traffic over several hours.  
In spite of its value, this kind of test should be reserved for the most critical cases due to the high cost in disruptions; the considerable expertise required in test planning and execution; and the risks associated with proper proof-level loading while measuring critical bridge responses. BOTH displacement and strain measurements were found to be essential in such a test rather than ONLY strain measurements. Unfortunately, most load tests are currently executed with only strain transducers. Parameter identification proved the relative value of displacements to strains and the writers recommend to use both types of measurements in any load test!
3. NDT applications were useful in revealing the variation in material properties and the extent of concrete deck delamination. NDT also indicated that delamination was NOT due to the corrosion of deck reinforcement. This leaves vibration as the probable cause discussed in the following. It is also important to note that NDT applications without vibration or load testing of the system are not as valuable as they are not sufficient for identifying damage or deterioration due to overlapping of multiple causes, and cannot help determine the capacity and possible failure modes of the system; Other experimental approaches, such as long-term monitoring, provided highly useful complementary insights but only since they followed from the structural identification exercise.
4. The research revealed that operational vibrations that are in the 20% g range are often detrimental to the serviceability and durability of a bridge, and the design of bridges should incorporate the effects of geometry on their vibration characteristics. Some of the amplifications due to vibration were attributed to the unusual

straight-skew geometry and the corresponding mode shapes. Dynamics obviously played a significant role in the deterioration of the deck as well as fatigue cracking, although proper design would have mitigated fatigue cracking.

5. Researchers conclude that a careful visual inspection by a professional bridge engineer who is equipped with excellent heuristics resulting from decades of practice could have observed and recorded all the damage and deterioration including the pier-cap crack. However, we have little heuristics in *bridge dynamics*, as bridges are designed, inspected, maintained and managed by assuming static behaviour. In design and rating, load effects are increased by an impact factor, but the levels of amplification that was interpreted for the test span would be higher if this simulation incorporated effects of bridge surface profile on truck inputs.
6. Perhaps the most important conclusion regards the necessity of measurements during bridge inspections. Accelerations, strains, tilts and displacements can now be measured by wireless sensors that may be quickly deployed, and operational monitoring of a bridge would reveal a wealth of understanding regarding the root causes of distresses and deteriorations [42]. Since we are fast losing the truly valuable experienced bridge engineers with heuristic knowledge, we should be making a transformation to objective metrics that will quantify the conditions and performance of a bridge. Given that the cost of typical overpasses often exceeds \$Tens of Millions, we cannot justify not demanding a new era of rational measurement of bridge performance and characteristics by objective performance and health indices in bridge engineering practice.
7. Regarding Conclusion 6, we should also recognize the fact that there are NOT many researchers and engineers who combine experience in experiment design and IT know-how along with a deep understanding of bridge structural engineering. While many professional entities do claim expertise in sensing and data acquisition, there is much more to claiming an ability to design and execute a field test so that measurement data may be trustworthy and can lead to interpretation and decision-making. The study reported in this paper brought such international experts together. However, when we consider widespread applications of field experiments that will yield meaningful data, we have to acknowledge the need for an extensive training and education program. Unfortunately, current business models for education and training in experimental arts by combining the physical laboratory and the field is not sufficient for widespread field measurement applications. Federal, State and local agencies have to work together to establish education and training on field experiments with reli-



able measurements. Otherwise we may only continue to discover only how little civil and bridge engineers really know about bridge behavior, performance and safety.

**Acknowledgements** This study was funded by the USDOT-FHWA and NJDOT as part of the Pilot Phase of FHWA's Long-Term Bridge Performance Program. The authors are deeply grateful to the contributions of their US-based academic collaborators Professors Franklin Moon, Jeff Weidner [56], Nenad Gucunski, Branko Glisic, Haluk Aktan, Marvin Halling as well as Yun Zhou, Jian Zhang and John Prader. FHWA researchers and officials Dr. Steven Chase and Dr. Hamid Ghasemi initiated the Long-Term Bridge Performance Program. Authors are especially grateful to International participants from Japan, Korea and Europe (Yozo Fujino, Tomonori Nagayama, Hyun-Moo Koh, Helmut Wenzel, James Brownjohn and Ian Smith as well as their teams) who generously supported and played very critical roles in this study. Finally, the senior authors deeply appreciate the current support and guidance by their FHWA colleagues Drs. Hoda Azari and David Kuehn. Additional information about this and other studies can be found on the "NDE Virtual Laboratory website" at: <http://vlab.asklab.net/VirtualLab/index.html>.

## References

1. ARTRB (2019) 2019 Bridge Report. [Online]. <https://artbabridgeport.org/reports/2019-ARTBA-Bridge-Report.pdf>. Accessed 1 Dec 2019.
2. Aktan AE, Brownjohn JMW (2013) Structural identification: opportunities and challenges. *ASCE J Struct Eng* 139:1639–1647. [https://doi.org/10.1061/\(ASCE\)ST.1943-541X.0000723](https://doi.org/10.1061/(ASCE)ST.1943-541X.0000723) (A special issue on Structural identification)
3. ASCE Technical Committee on Structural Identification (2013) Structural identification of constructed systems: approaches, methods, and technologies for effective practice of St-Id. In: Çatbas FN, Kijewski-Correa T, Aktan AE (eds). *ASCE*. pp 1–248. <https://doi.org/10.1061/9780784411971>
4. Bertero V, Aktan A, Charney F, Sause R (1985) Earthquake simulator tests and associated experimental, analytical, and correlation studies of one-fifth scale model, Earthquake effects on reinforced concrete structures, U.S.–Japan Research, ACI Special Publication SP-84, American Concrete Institute, Detroit, pp 375–424
5. Aktan EA, Farhey DN (1996) Condition and reliability assessment of constructed facilities. Spec. Publ. No. 162, American Concrete Institute, Detroit, pp 73–92
6. Aktan AE, Farhey DN, Helmicki AJ, Brown DL, Hunt VJ, Lee KL, Levi A (1997) Structural identification for condition assessment: experimental arts. *J Struct Eng ASCE*. 123(12):1674–1684. [https://doi.org/10.1061/\(ASCE\)0733-9445\(1997\)123:12\(1674\)](https://doi.org/10.1061/(ASCE)0733-9445(1997)123:12(1674))
7. Aktan AE, Catbas N, Turer A, Zhang Z (1998) Structural identification: analytical aspects. *J Struct Eng ASCE* 124(7). [https://doi.org/10.1061/\(ASCE\)0733-9445\(1998\)124:7\(817\)](https://doi.org/10.1061/(ASCE)0733-9445(1998)124:7(817))
8. Farrar C, Cornwell P, Doebling S, Prime M (2000) Structural health monitoring studies of the alamosa canyon and I-40 bridges. United States. <https://doi.org/10.2172/766805>. <https://www.osti.gov/servlets/purl/766805>
9. Peeters B, De Roeck G (2001) One-year monitoring of the Z24-Bridge: environmental effects versus damage events. *Earthq Eng Struct Dyn* 30(2):149–171. [https://doi.org/10.1002/1096-9845\(200102\)30:2<149::AID-EQE1>3.0.CO;2-Z](https://doi.org/10.1002/1096-9845(200102)30:2<149::AID-EQE1>3.0.CO;2-Z)
10. Catbas N, Lenett M, Aktan A, Brown D, Helmicki A, Hunt V (1998) Damage detection and condition assessment of seymour bridge. In: Proceedings of the 16th international modal analysis conference, Society of Experimental Mechanics, Bethel, Conn., pp 1694–1702
11. Ciloglu K, Zhou Y, Moon FL, Aktan AE (2012) Impacts of epistemic uncertainty in operational modal analysis. *J Eng Mech* 138(9):1059–1070
12. Grimmelsman KA (2006) Experimental characterization of towers in cable-supported bridges by ambient vibration testing. Doctoral Thesis, Drexel University. <http://hdl.handle.net/1860/1222>
13. Pan Q (2007) System identification of constructed civil engineering structures and uncertainty. Doctoral Thesis, Drexel University. <http://hdl.handle.net/1860/2531>
14. Grimmelsman KA, Pan Q, Aktan AE (2007) Analysis of data quality for ambient vibration testing of the henry hudson bridge. *J Intell Mater Syst Struct* 18(8):765–775. <https://doi.org/10.1177/1045389X06074774>
15. Friswell M, Mottershead J (1995) Finite element model updating in structural dynamics (Solid Mechanics and Its Applications). Kluwer Academic Publishers, London
16. Mottershead JE, Friswell MI (1993) Model updating in structural dynamics: a survey. *J Sound Vib* 167(2):347–375
17. Friswell MI, Inman DJ, Pilkey DF (1998) Direct updating of damping and stiffness matrices. *AIAA J* 36(3):491–493. <https://doi.org/10.2514/2.396>
18. Levin RI, Lieven NAJ (1998) Dynamic finite element model updating using simulated annealing and genetic algorithms. *Mech Syst Signal Process* 12(1):91–120. <https://doi.org/10.1006/mssp.1996.0136>
19. Minshui H, Hongping Z (2008) Finite element model updating of bridge structures based on sensitivity analysis and optimization algorithm. *Wuhan Univ J Nat Sci* 13(1):87–92. <https://doi.org/10.1007/s11859-008-0117-1>
20. Bakir PG, Reynders E, De Roeck G (2007) Sensitivity-based finite element model updating using constrained optimization with a trust region algorithm. *J Sound Vib* 305(1–2):211–225. <https://doi.org/10.1016/J.JSV.2007.03.044>
21. Law K (1997) A Bayesian probabilistic approach for structure damage detection. *Earthq Eng Struct Dyn* 26:1259–1281. [https://doi.org/10.1002/\(SICI\)1096-9845\(199712\)26:12%3c1259::AID-EQE709%3e3.0.CO;2-3](https://doi.org/10.1002/(SICI)1096-9845(199712)26:12%3c1259::AID-EQE709%3e3.0.CO;2-3)
22. Prajapat K, Ray chaudhuri S (2016) Prediction error variances in bayesian model updating employing data sensitivity. *J Eng Mech* 142:4016096. [https://doi.org/10.1061/\(ASCE\)EM.1943-7889.0001158](https://doi.org/10.1061/(ASCE)EM.1943-7889.0001158)
23. Prajapat K, Raychaudhuri S (2016) Posterior resolution and structural modification for parameter determination in bayesian model updating. *Int J Cybern Informatics* 5:193–202. <https://doi.org/10.5121/ijci.2016.5118>
24. Yallee RB, Young RJ, Katafygiotis L, Papadimitriou C, Lam HF (1998) A probabilistic approach to structural model updating. *Soil Dyn Earthq Eng* 17(7–8):495–507. [https://doi.org/10.1016/S0267-7261\(98\)00008-6](https://doi.org/10.1016/S0267-7261(98)00008-6)
25. Marwala T, Mdlazi L, Sibisi S (2007) Finite element model updating using bayesian approach. arXiv preprint [arXiv :0705.2515](https://arxiv.org/abs/0705.2515)
26. Behmanesh I, Moaveni B, Lombaert G, Papadimitriou C (2015) Hierarchical Bayesian model updating for structural identification. *Mech Syst Signal Process* 64–65:360–376. <https://doi.org/10.1016/J.YMSSP.2015.03.026>
27. Vanik MW, Beck JL, Au SK (2000) Bayesian probabilistic approach to structural health monitoring. *J Eng Mech* 126(7):738–745. [https://doi.org/10.1061/\(ASCE\)0733-9399\(2000\)126:7\(738\)](https://doi.org/10.1061/(ASCE)0733-9399(2000)126:7(738))

28. Beck JL, Katafygiotis LS, B. J. L., K. L. S. (1998) Updating models and their uncertainties. I: bayesian statistical framework. *J Eng Mech* 124(4):455–461. doi: 10.1061/(ASCE)0733-9399(1998)124:4(455).
29. Zhang J, Guo SL, Wu ZS, Zhang QQ (2015) Structural identification and damage detection through long-gauge strain measurements. *Eng Struct* 99:173–183. <https://doi.org/10.1016/J.ENGSTRUCT.2015.04.024>
30. Noël JP, Kerschen G (2017) Nonlinear system identification in structural dynamics: 10 more years of progress. *Mech Syst Signal Process* 83:2–35. <https://doi.org/10.1016/J.YMSSP.2016.07.020>
31. Hearn G, Testa RB (1991) Modal analysis for damage detection in structures. *J Struct Eng* 117(10):3042–3063. [https://doi.org/10.1061/\(ASCE\)0733-9445\(1991\)117:10\(3042\)](https://doi.org/10.1061/(ASCE)0733-9445(1991)117:10(3042))
32. Salawu OS (1997) Detection of structural damage through changes in frequency: a review. *Eng Struct* 19(9):718–723. [https://doi.org/10.1016/S0141-0296\(96\)00149-6](https://doi.org/10.1016/S0141-0296(96)00149-6)
33. Ren W-X, Zhao T, Harik IE (2004) Experimental and analytical modal analysis of steel arch bridge. *J Struct Eng* 130(7):1022–1031. [https://doi.org/10.1061/\(ASCE\)0733-9445\(2004\)130:7\(1022\)](https://doi.org/10.1061/(ASCE)0733-9445(2004)130:7(1022))
34. Gentile C, Saisi A (2007) Ambient vibration testing of historic masonry towers for structural identification and damage assessment. *Constr Build Mater* 21(6):1311–1321. <https://doi.org/10.1016/J.CONBUILDMAT.2006.01.007>
35. Doebling SWS, Farrar CCR, Prime MMB, Doebling SWS, Farrar CCR, Prime MMB (1998) A summary review of vibration-based damage identification methods. *Shock Vib Dig* 30:1–34
36. Doebling SW, Farrar CR, Prime MB, Shevitz DW (1996) Damage identification and health monitoring of structural and mechanical systems from changes in their vibration characteristics: a literature review, Los Alamos, NM
37. Farrar CR, Doebling SW, Nix DA (2001) Vibration-based structural damage identification. *Philos Trans R Soc A Math Phys Eng Sci* 359(1778):131–149. <https://doi.org/10.1098/rsta.2000.0717>
38. Sohn H et al (2004) A review of structural health monitoring literature : 1996–2001, technical report. Report number LA-13976-MS.
39. Bartoli G, Betti M, Facchini L, Marra A, Monchetti S (2017) Bayesian model updating of historic masonry towers through dynamic experimental data. *Procedia Eng* 199:1258–1263. <https://doi.org/10.1016/j.proeng.2017.09.267>
40. Pepi C, Gioffre M, Grigoriu MD (2019) Parameters identification of cable stayed footbridges using Bayesian inference. *Meccanica* 54(9):1403–1419. <https://doi.org/10.1007/s11012-019-01019-x>
41. Chase SB, Adu-Gyamfi Y, Aktan AE, Minaie E (2016) Synthesis of national and international methodologies used for bridge health indices. Publication No. FHWA-HRT-15-081. <https://doi.org/10.13140/RG.2.1.1558.1683>
42. Aktan AE, Bartoli I, Karaman SG (2019) Technology leveraging for infrastructure asset management: challenges and opportunities. *Front Built Environ* 5:61. <https://doi.org/10.3389/fbuil.2019.00061>
43. DASSAULT SYSTÈMES, ABAQUS UNIFIED FEA, *SIMULIA web site*. [Online] <https://www.3ds.com/products-services/simulia/products/abaqus/>. Accessed 1 Oct 2019
44. MathWorks, “fminsearch,” The MathWorks, Inc. [Online]. <https://www.mathworks.com/help/optim/ug/fminsearch-algorithm.html>. Accessed 1 Oct 2019
45. AASHTO, AASHTO LRFD bridge design specifications. Fourth edition with 2008 interim revisions. Washington, D.C. : American Association of State Highway and Transportation Officials, [2008] ©2007, 2010.
46. Law SS, Zhu XQ (2004) Dynamic behavior of damaged concrete bridge structures under moving vehicular loads. *Eng Struct* 26(9):1279–1293. <https://doi.org/10.1016/j.engstruct.2004.04.007>
47. Kim C (2005) Three-dimensional dynamic analysis for bridge-vehicle interaction with roadway roughness. *Comput Struct* 83(19):1627–1645. <https://doi.org/10.1016/j.comptruc.2004.12.004> **Pergamon Press, [Oxford]**
48. Kalyankar R, Uddin N (2016) Simulating the effects of surface roughness on reinforced concrete t beam bridge under single and multiple vehicles. *Adv Acoust Vib* 2016:3594148. <https://doi.org/10.1155/2016/3594148>
49. Frýba Ladislav (1973) Vibration of solids and structures under moving loads. <https://doi.org/10.1007/978-94-011-9685-7>
50. Paultre P, Chaallal O, Proulx J (1992) Bridge dynamics and dynamic amplification factors—a review of analytical and experimental findings. *Can J Civ Eng* 19(2):260–278. <https://doi.org/10.1139/192-032>
51. Brady S, Obrien E, Znidaric A (2006) Effect of vehicle velocity on the dynamic amplification of a vehicle crossing a simply supported bridge. *J Bridg Eng* 11(2):241–249. [https://doi.org/10.1061/\(ASCE\)1084-0702\(2006\)11:2\(241\)](https://doi.org/10.1061/(ASCE)1084-0702(2006)11:2(241))
52. Kou J-W, DeWolf J (1997) Vibrational behavior of continuous span highway bridge—influencing variables. *J Struct Eng* 123:333–344. [https://doi.org/10.1061/\(ASCE\)0733-9445\(1997\)123:3\(333\)](https://doi.org/10.1061/(ASCE)0733-9445(1997)123:3(333))
53. Meng JY, Lui E, Liu Y (2001) Dynamic response of skew highway bridges. *J Earthq Eng* 5:205–223. <https://doi.org/10.1080/13632460109350392>
54. Deng L, Yu Y, Zou Q, Cai C (2014) State-of-the-art review of dynamic impact factors of highway bridges. *J Bridg Eng* 20:4014080. [https://doi.org/10.1061/\(ASCE\)BE.1943-5592.0000672](https://doi.org/10.1061/(ASCE)BE.1943-5592.0000672)
55. Braley J (2019) Understanding vehicle-bridge interaction through field measurements and model-based simulations. Doctoral Thesis. Rutgers, The State University of New Jersey
56. Weidner J (2012) Structural identification of a complex structure using both conventional and multiple model approaches. Doctoral Thesis. Drexel University. <http://hdl.handle.net/1860/3818>

**Publisher's Note** Springer Nature remains neutral with regard to jurisdictional claims in published maps and institutional affiliations.